CHAPTER 7

ORE MINERAL TEXTURES

7.1 INTRODUCTION

Ore microscopy involves not only the identification of individual mineral grains but also the interpretation of ore mineral textures, that is, the spatial relationships between grains. Barton (1991) has astutely noted that "the interpretation of textures is simultaneously one of the most difficult and important aspects of the study of rocks and ores." Textures may provide evidence of the nature of such processes as initial ore deposition, postdepositional re-equilibration or metamorphism, deformation, annealing, and meteoric weathering. The recognition and interpretation of textures is often the most important step in understanding the origin and postdepositional history of an ore. However, the extent to which the ore minerals retain the compositions and textures formed during initial crystallization varies widely. Figure 7.1 illustrates this variability in terms of equilibration rates and shows that oxides, disulfides, arsenides, and sphalerite are the most refractory of ore minerals. These minerals are more likely to preserve evidence of their original conditions of formation than are minerals such as the pyrrhotites or Cu-Fe sulfides. Argentite, sulfosalts, and native metals are among the most readily re-equilibrated ore minerals and thus are the least likely to reflect initial formation conditions. The textures observed in many polymetallic ores reflect the stages, sometimes numerous, in their development and postdepositional history. Consequently, the textures and compositions observed in close proximity in complex polymetallic ores may actually reflect several different stages in the development and postdepositional history of an ore deposit. Hence, the morphologies and inclusion patterns within refractory minerals such as pyrite may represent initial high-temperature conditions, whereas coexisting pyr-
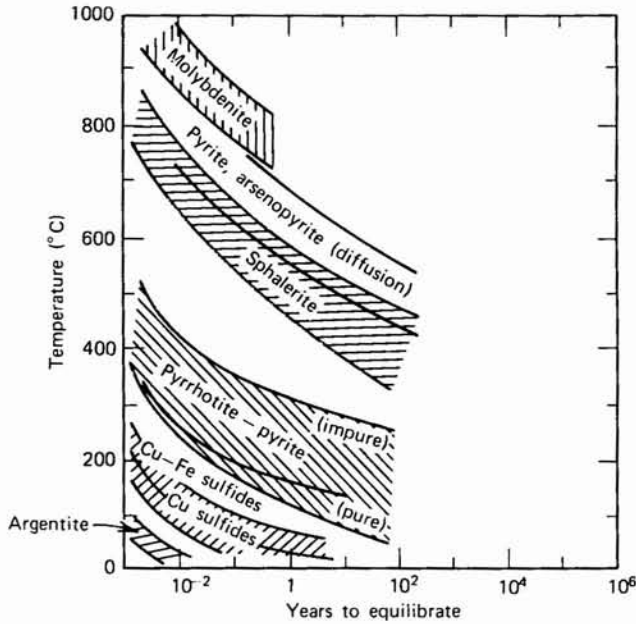
FIGURE 7.1   Equilibration times for various sulfides involved in solid state reactions. The field widths represent differing rates in different reactions, as well as changes in rates due to compositional differences in a phase and a great deal of experimental uncertainty. (From H. L. Barnes, *Geochemistry of Hydrothermal Ore Deposits*, 2nd ed., copyright © 1979, Wiley-Interscience, New York, p. 287; used with permission.)

rhotites may have equilibrated-to-intermediate-temperature conditions during cooling, and minor sulfosalts or native metals may have equilibrated down to the very lowest ambient temperatures. Furthermore, there are often weathering effects that have been superimposed much later and that may be totally unrelated to the original processes of formation. Hence, complete textural interpretation involves not only recognition and interpretation of the individual textures but also their placement in the time framework of the evolution of the deposit from its formation until the present day.

Textural recognition and interpretation, in addition to providing insight into the history of a deposit, may also aid in mineral identification (see Section 3.5) and may supply information valuable to ore milling and beneficiation. Furthermore, the same textures observed in ore mineral assemblages are found in a large variety of synthetic-made materials (e.g., slags, metals, dental amalgams, corrosion products), and proper interpretation can help in the solution of many practical problems. Several of these aspects are discussed in Chapter 11.

It is not possible, in this text, to discuss the complete variety of textures observed in ores, but a number of common examples will be described and used to illustrate the principles involved in textural interpretation. Many

additional textures found in specific ore associations are illustrated in Chapters 9 and 10. It is worth noting that many textures are still inadequately understood and that experienced ore microscopists still disagree as to their precise origin. Clearly, there remains much to be learned in the realm of textural interpretation.
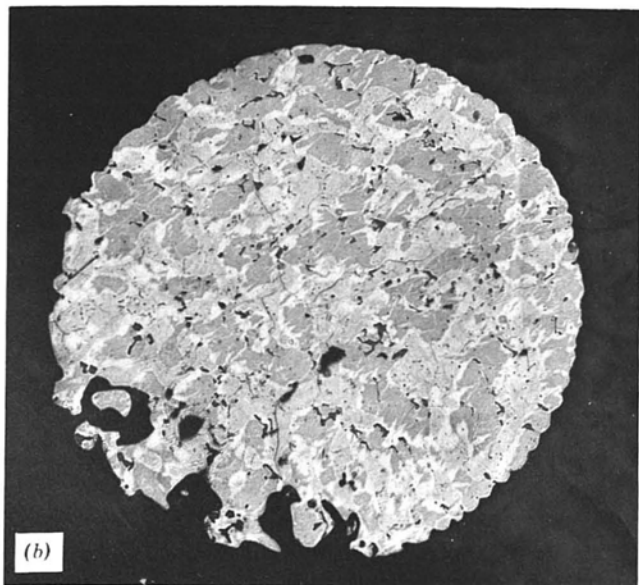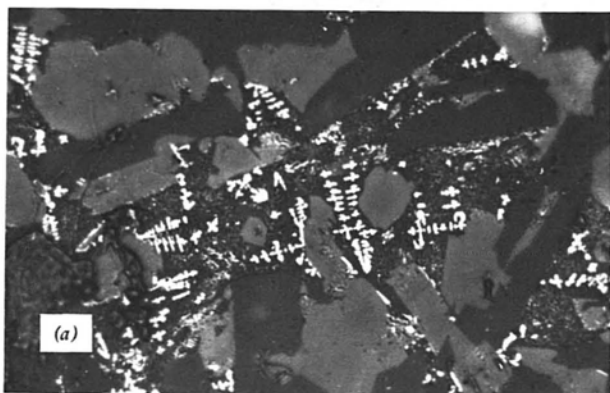

FIGURE 7.2   (*a*) Skeletal crystals of ilmenite in basalt from Hawaii (width of field = 150 μm). (*b*) Sulfide droplet in Mid-Atlantic Ridge basalt, composed of $(Fe,Ni)_{1-x}S$ monosulfide solid solution (medium gray) and $(Cu, Fe)S_{2-x}$ intermediate solid solution (light gray), with rims and flames of pentlandite (bright) (width of field = 250 μm). (Reproduced from G. K. Czamanskie and J. G. Moore, *Geol. Soc. Amer. Bull.* **88**, 591, 1977, with permission.)

7.2 PRIMARY TEXTURES OF ORE MINERALS FORMED FROM MELTS

The growth of ore minerals in silicate melts generally results in the development of euhedral to subhedral crystals, because there is little obstruction to the growth of faces. Thus, primary chromite, magnetite, ilmenite, and platinum minerals, phases that are refractory enough to retain original textures, often occur as well-developed equant euhedra interspersed in the plagioclase, olivine, and pyroxene of the host rock (Figure 9.1). Unobstructed growth, especially in rapidly cooled basalts, sometimes results in the formation of skeletal crystals (Figure 7.2a) that may be wholly or partially contained within subsequently solidified glasses or crystallizing silicates. Poikilitic development of silicates in oxides or oxides in silicates is not uncommon. In oxide-rich layers, the simultaneous crystallization of mutually interfering grains results in subhedral crystals with widely variable interfacial angles. In contrast, the interfacial angles at triple-grain junctions of monomineralic masses that have been annealed during slow cooling or during metamorphism generally approach 120° (see Section 7.7 for further discussion).

Iron (plus nickel, copper)-sulfur (-oxygen) melts, from which iron-nickel-copper ores form (see Section 9.3), generally crystallize later than the enclosing silicates. The magnetite often present in these ores crystallizes, whereas the iron sulfides are wholly or partially molten, and thus tends to be euhedral or skeletal, whereas the much less refractory sulfides (mostly pyrrhotite) exhibit textures of cooling and annealing. Primary iron-sulfur (-oxygen) melts can also result in the formation of small (<100 μm) round droplets trapped in rapidly cooled basalts and basaltic glasses (see Figure 7.2b).

7.3 PRIMARY TEXTURES OF OPEN-SPACE DEPOSITION

The initial deposition and growth of the ore and gangue minerals in many deposits occurs in open spaces in vugs or fractures developed by dissolution or during faulting. Although the open space may no longer be evident because of subsequent infilling or deformation, the initial formation of the crystals in open space is often still evidenced by the presence of well-developed crystal faces (especially in such minerals as sphalerite—see Figures 7.3a and 7.3b—or chalcopyrite that rarely exhibit euhedral forms), by crystals that exhibit growth-zoning (Figure 7.4), by colloform or zoned monomineralic bands (Figures 7.5a–7.5c). All of these features result from unobstructed growth of minerals into fluid-filled voids, the banding being the result of a change in the ore-forming fluids and the physico-chemical environment of mineralization with time. Deposition from hydrothermal solutions in open fissures can result in *comb structures* and in *symmetrically* and *rhythmically* crustified veins, as shown in Figures 7.6a and 7.6b. Movement along such a vein during or after ore formation may cause brecciation resulting in *breccia* ore (Figure 7.7). All of

(a)
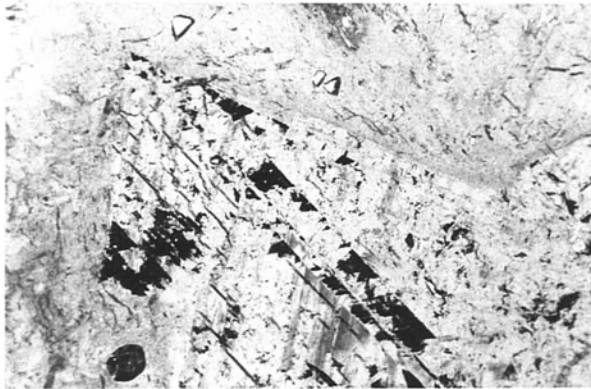
· (b)

FIGURE 7.3 (*a*) Well-developed freestanding crystals such as these 1–2 cm diameter sphalerites are generally good evidence of growth in open spaces, Elmwood, Tennessee (centimeter scale). (*b*) The face of the first generation of sphalerite (containing numerous dark fluid inclusions) cuts across from the upper left to the lower right portion of the photograph. The second generation of sphalerite, which fills the upper portion of the photograph, contains few inclusions and a much lower level of trace constituents. Doubly polished thin section; Elmwood, Tennessee (width of field = 1,400 µm).

these textures may be developed on a scale ranging from macroscopic to microscopic, and their recognition is important if one is trying to reconstruct the entire paragenetic history of a deposit. Open-space filling is exemplified by the Cu-Pb-Zn(-Ag) vein deposits (discussed in Section 9.6) composed of pyrite, sphalerite, galena, chalcopyrite, and silver-bearing sulfosalts, and by some Pb-Zn ores in carbonates (discussed in Section 10.7). Pyrite in these ores generally forms as isolated cubes, more rarely as octahedra or pyritohedra, or as aggregates of interfering crystals along the walls of fractures. Sphalerite may occur as honey-yellow to black crystals or radiating colloform aggregates,
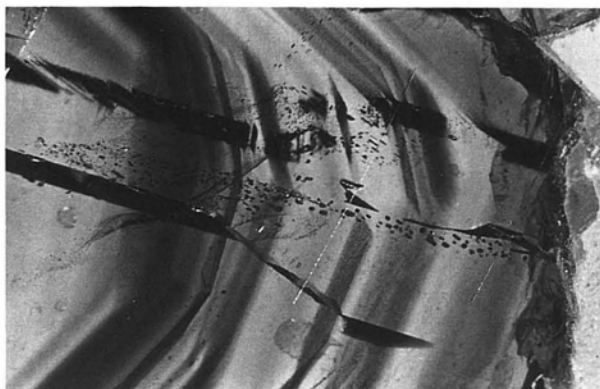
FIGURE 7.4 Growth zoning in a single crystal of sphalerite (from Creede, Colorado) viewed in transmitted light through a doubly polished thin section. Trails of fluid inclusions are visible cutting across the growth zones (width of field = 1,200 μm).
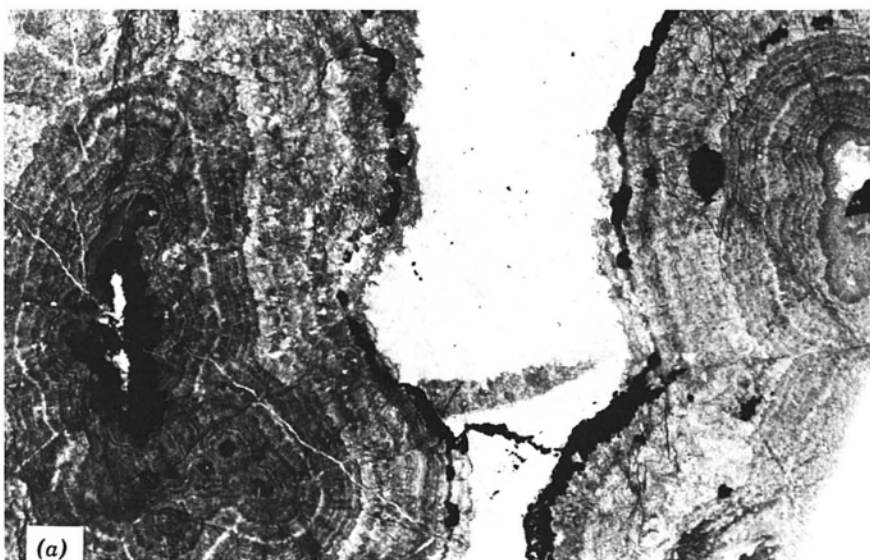

(a)

FIGURE 7.5 (a) Concentric growth banding in sphalerite (from Austinville, Virginia) viewed in transmitted light through a doubly polished thin section. Black areas are pyrite; white areas are dolomite (width of field = 4 cm). (b) Colloform growth banding in sphalerite (from Pine Point, North West Territories, Canada) seen in reflected light (width of field = 2 cm). (c) Growth zoning in pyrite showing radial and concentric development (from Ainai Mine, Japan) seen in reflected light (width of field = 2,000 μm).
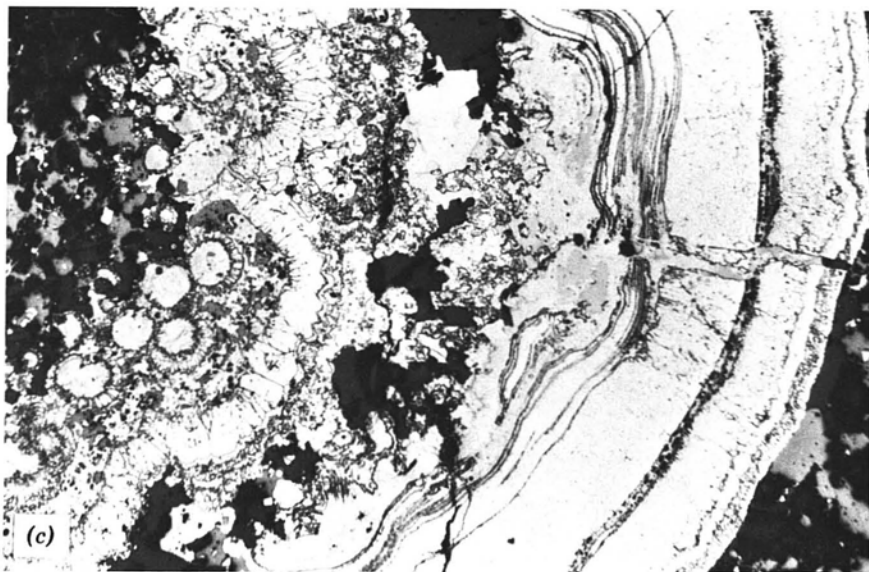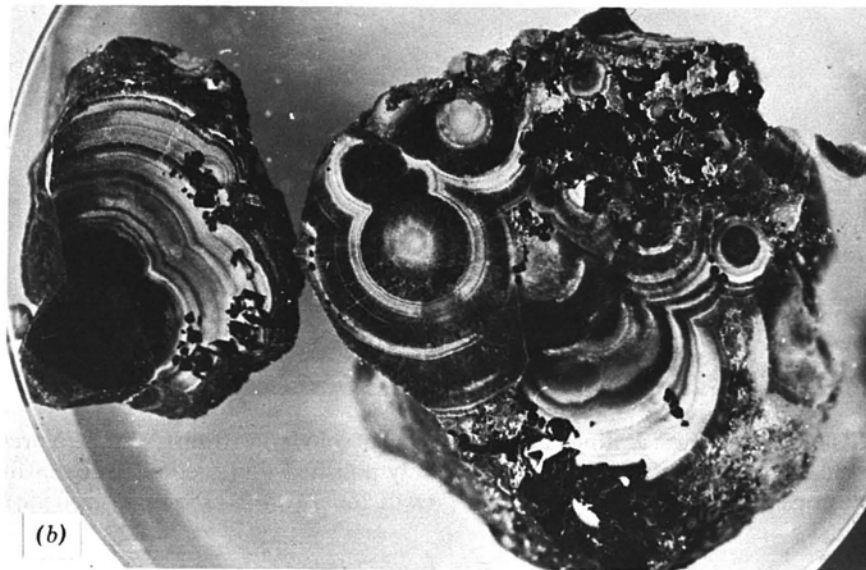
FIGURE 7.5 (*Continued*)

which often contain a well-developed growth banding or zoning (Figure 7.4); this structure is clearly visible in doubly polished thin sections but is difficult to see in polished sections (see Section 2.5 and Figure 2.9). Darker sphalerite colors generally indicate higher iron content, but this correlation is by no means consistent and is especially unreliable if iron content is below 5%. Galena, commonly observed as anhedral intergranular aggregates in many
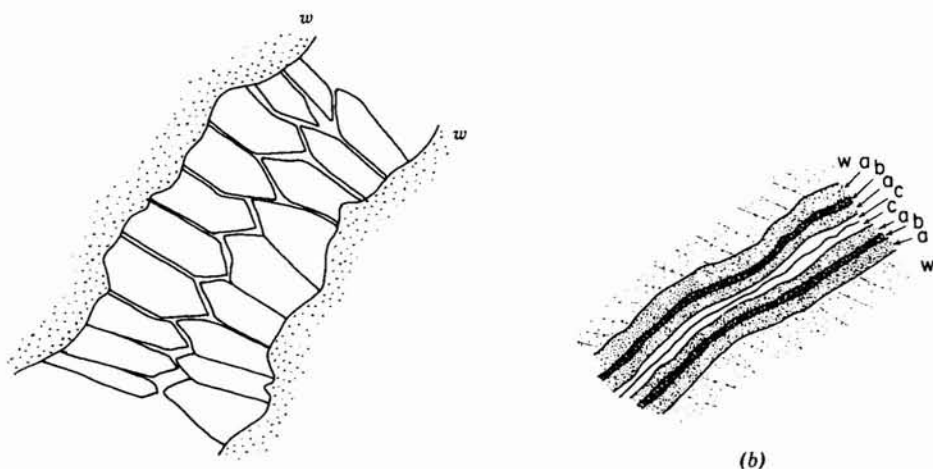
FIGURE 7.6 (*a*) Comb structure showing growth of crystals outward from fracture walls. (*b*) Symmetrically crustified vein showing successive deposition of minerals inward from open fracture walls. This vein is also rhythmically crustified in showing the depositional sequences *a-b-a-c* (*w* = wall rock). Scale variable from millimeter to several meters across vein.

types of ores, often occurs as well-formed cubes and less commonly as octahedra or skeletal crystals in open voids. Episodic precipitation, sometimes with intervening periods of leaching, often leaves hopper-like crystals of galena. Chalcopyrite, tetrahedrite, and the "ruby-silvers" (polybasite-pearcite), which almost never exhibit any crystal form in massive ores, commonly appear as euhedral crystals when unimpeded growth in open cavities occurs.
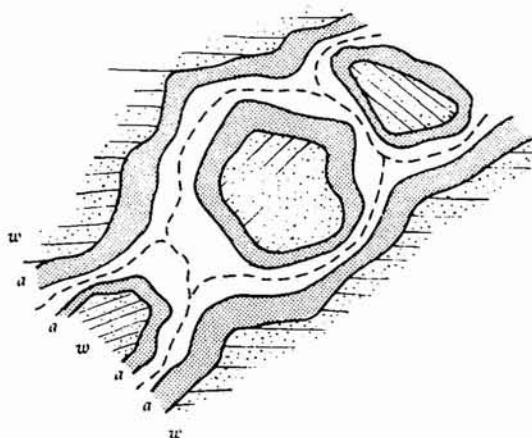

FIGURE 7.7   Breccia ore showing successive deposition of minerals on breccia fragments and other wall rocks. Scale variable from wall rock fragments of millimeter to several meters across breccia fragments.
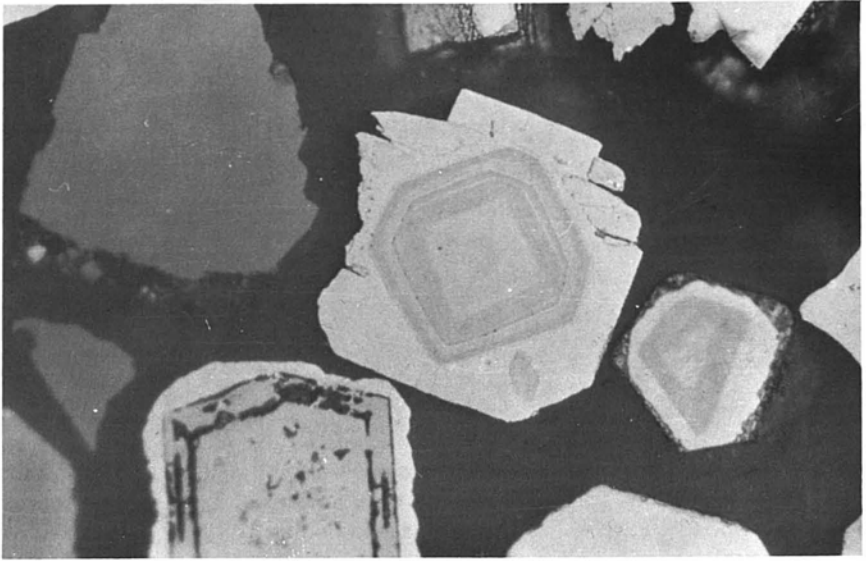
FIGURE 7.8 Compositionally zoned crystals of bravoite (Fe,Ni,Co)S_2 from Maubach, Germany (width of field = 60 µm).

(a)

FIGURE 7.9 (a) Radiating fibrous crystals of the manganese oxide mineral chalcophanite infilling an open fracture, Red Brush Mine, Virginia (width of field = 2,000 µm). (b) Radiating clusters of fibrous goethite crystals forming a botryoidal aggregate in a weathering zone, Giles Co., Virginia (width of field = 2,000 µm).
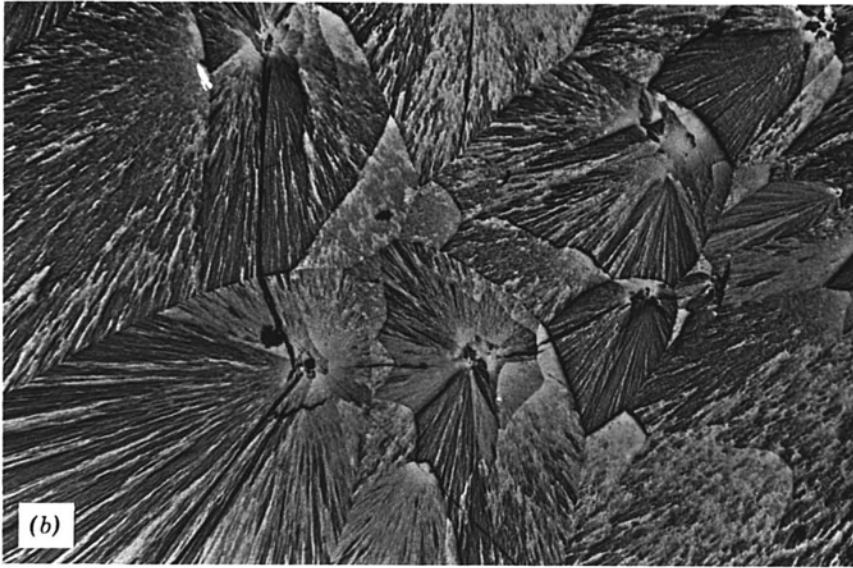
FIGURE 7.9   (*Continued*)

Sequential deposition from cobalt- and nickel-bearing solutions may result in the development of concentrically growth-zoned pyrite-bravoite crystals (Figure 7.8), which often reveal changing crystal morphology (cube, octahedron, pyritohedron) during growth. A similar process of sequential deposition from metal- and sulfur-bearing fluids circulating through the intergranular pore spaces in sediments may leave concentric sulfide coatings on the sediment grains.

Iron and manganese oxides and hydroxides often form botryoidal or even stalactitic structures in open fractures as a result of meteoric water circulation. These minerals (e.g., goethite, lepidocrocite, pyrolusite, cryptomelane) may form concentric overgrowths inward from vein walls or complex masses of fibrous (brush-like) crystals (Figures 7.9a and 7.9b) radiating from multiple growth sites along an open fracture.

"Colloform" textures (see Figure 7.5b) have often been cited as evidence for initial formation by colloidal deposition; however, Roedder (1968) has shown that many colloform sphalerites in Pb-Zn ores (see Section 8.2.3) grew as tiny fibrous crystals projecting into a supersaturated ore fluid.

7.4   SECONDARY TEXTURES RESULTING FROM REPLACEMENT (INCLUDING WEATHERING)

Replacement of one ore mineral by another or by a mineral formed during weathering is common in many types of ores. However, a major problem in textural interpretation is the recognition of replacement when no vestige of the

replaced phase remains. Probably the most easily recognized replacement textures are those in which organic materials, such as wood fragments (Figures 7.10a and 10.7) or fossil shells have been pseudomorphed by metal sulfides (commonly pyrite, marcasite, chalcocite) or oxides (commonly hematite, goethite, "limonite," uranium minerals) (Figure 7.10b). Pyrite cubes and marcasite laths that have been replaced by iron oxides during weathering (Figure 7.10c) are also readily identified.

Replacement may result from one or more of the following processes: (1) dissolution and subsequent reprecipitation, (2) oxidation, and (3) solid state diffusion. The resulting boundary between the replaced and the replacing mineral is commonly either sharp and irregular (a *careous*, or corroded texture) or *diffuse*.

Edwards (1947), Bastin (1950), and Ramdohr (1969) have described a wide variety of replacement geometries—rim, zonal, frontal, and so on—but they all appear to represent variations of the same process. Replacement textures depend chiefly for their development on three features of the phase being replaced: (1) the surfaces available for reaction, (2) the crystal structures of the
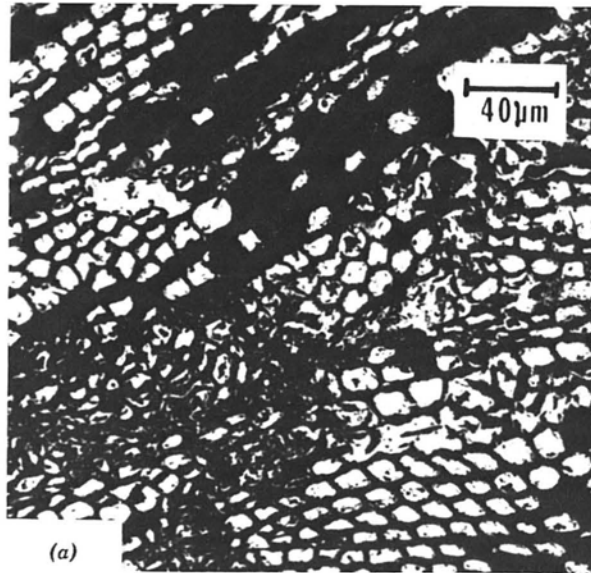

(a)

FIGURE 7.10   (a) Cellular structure in coal material replaced by pyrite, Minnehaha Mine, Illinois (width of field = 270 μm). (Reproduced from F. T. Price and Y. N. Shieh, *Econ. Geol.* **74**, 1448, 1979, with permission of the authors and the publisher.) (b) Pseudomorphous replacement of euhedral marcasite (white) crystals by goethite (light gray), Northern Pennine Orefield, England (width of field = 500 μm). (c) Pyrite cubes have been converted into goethite during weathering with the formation of a relatively solid outer rim and a porous interior, Morning Star Mine, California (width of field = 1,200 μm). (Photograph by R. W. Sheets.)
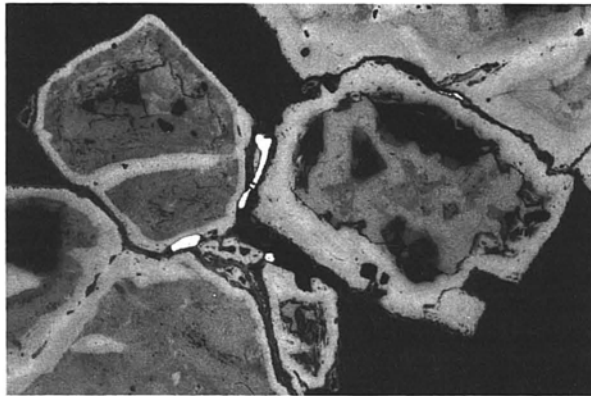
FIGURE 7.10   (*Continued*)

original and secondary minerals, and (3) the chemical compositions of the
original mineral and the reactive fluid.

7.4.1   Crystal Surfaces

Replacement is the result of a surface chemical reaction; hence, any channel
between grains or through grains is a prime site for initiation of the replace-
ment process. Replacement along grain boundaries or internal channel ways
very often appears in the form of thin laths or equant crystals of the replacing
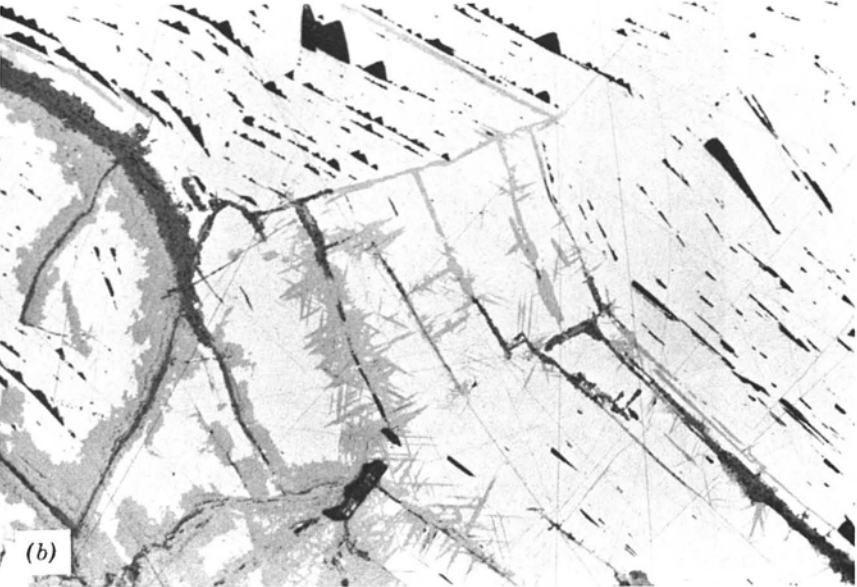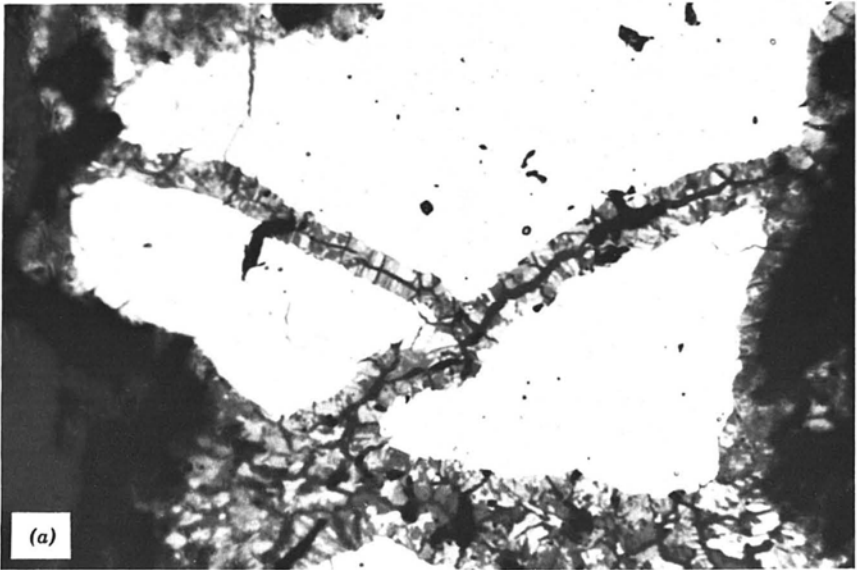
FIGURE 7.11   (a) Covellite replacing chalcopyrite (white) along grain boundaries, Great Gossan Lead, Virginia (width of field = 520 μm). (b) Chalcocite (medium gray) replacing galena (light gray) along grain boundaries and cleavages, Alderley Edge, Cheshire, England (width of field = 500 μm). (c) Galena (white) replaced by cerussite ($PbCO_3$, light gray) from the margins of the original grain, Northern Pennine Orefield, England (width of field = 500 μm). (d) Fine-grained pyrite and marcasite (white)
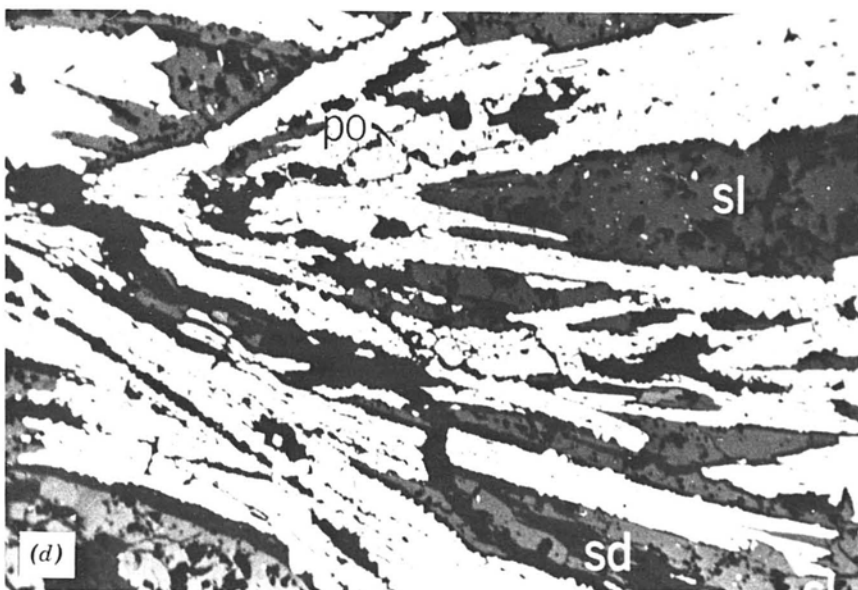
pseudomorphously replacing elongated crystals of pyrrhotite. Some remnants of pyrrhotite (po) remain in the cores of these pseudomorphs. Sphalerite (sl) and siderite (sd) comprise the matrix (width of field = 3,000 μm). (Reproduced from W. C. Kelly and F. S. Turneaure, *Econ. Geol.* **65**, 620, 1970, with permission of the authors and the publisher.)

phase projecting into the host. It may also appear as thin concentric coatings developed roughly parallel to the advancing front of replacement. In the early stages of the process, replacement may be readily identified, because much of the original phase remains and the original grain boundaries, fractures, or cleavages are still visible (Figures 7.11a and 7.11b). In more advanced stages, the original phase may be reduced to "islands" now left in a matrix of the secondary minerals (Figure 7.11c). If the original material was coarsely crystalline and optically anisotropic, the residual island grains may well show optical continuity (i.e., extinguish simultaneously when viewed under crossed polars). Complete replacement of one mineral by another is often difficult to establish unless vestigial structures, such as the typical morphology of the replaced phase (pyrite cubes now seen as goethite, Figure 7.10c; pyrrhotite laths now seen as pyrite and marcasite, Figure 7.11d), are left behind.

With careful observation, one can usually distinguish between replacement along fractures and mere fracture infilling resulting from precipitation of a later phase or its injection during metamorphism. Replacement consumes some of the original phase and tends to produce a rounding off of irregular surfaces, whereas infilling leaves the original fractured surfaces intact. After replacement, the surfaces on either side of a fracture do not "match" (Figure 7.12a), whereas, after infilling, the surfaces should still "match" (Figure 7.12b). It is important to note that textures such as that shown in Figure 7.12b have been erroneously interpreted and used as evidence that pyrite is breaking down to form pyrrhotite in these ores.

Replacement along fractures may also resemble some of the exsolution textures discussed later. However, replacement commonly results in an increase in the volume of the secondary replacing phase at the intersections of fractures, whereas this is not common in exsolution. In fact, exsolution often produces the opposite effect in which intersecting exsolution lamellae show depletion of the exsolved phase in the zone of intersection. For the same reasons, exsolution often leaves depleted zones in the host phase (Figure 7.17d) adjacent to major concentrations of the exsolved phase. Replacement, however, may result in greater concentration of the secondary phase adjacent to, and extending out from, major replacement areas.

7.4.2   Crystal Structures

The crystal structure of the phase being replaced may control replacement, either because this determines cleavage directions or because diffusion can take place more readily along certain crystallographic directions. For example, the oxidation of magnetite commonly results in replacement by hematite along (111) planes (Figure 7.34).

7.4.3   Chemical Composition

The chemical composition of the primary phase may control the composition of the phase that replaces it. During weathering, and often during hydrother-

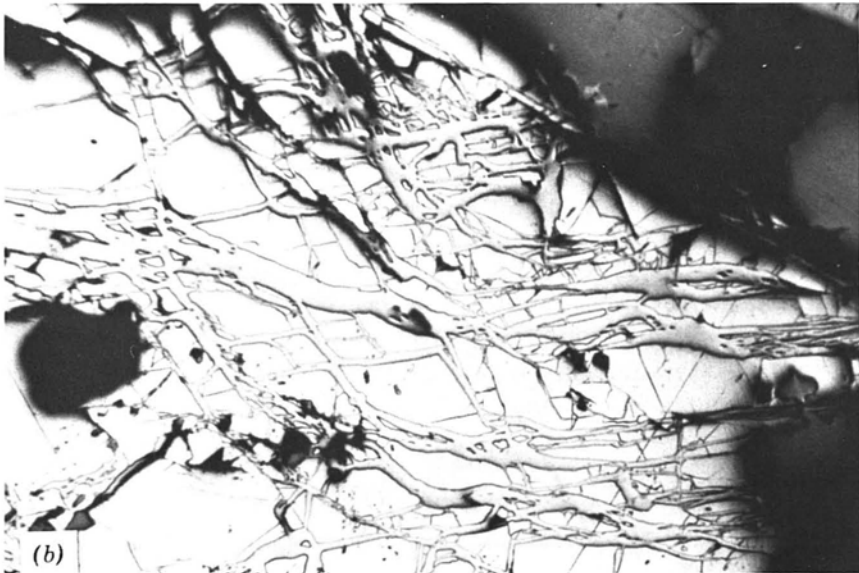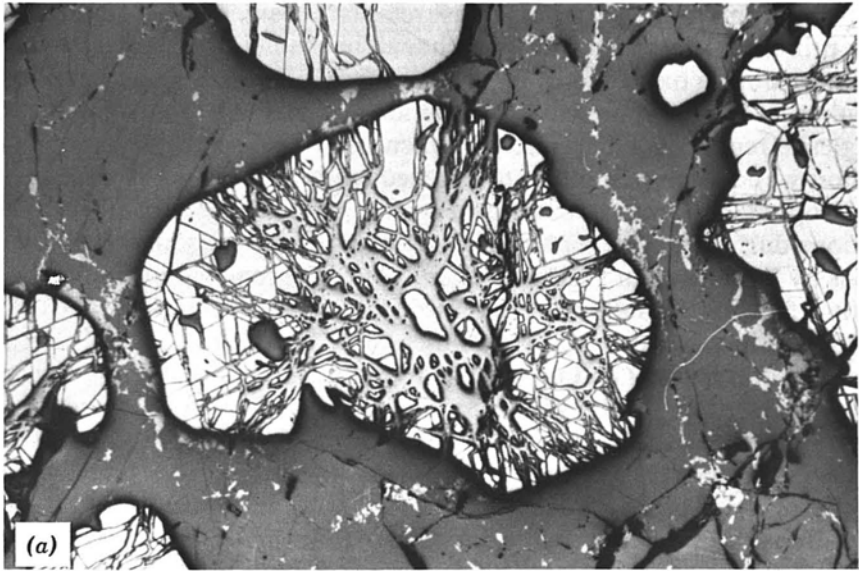**FIGURE 7.12** (*a*) Subhedral pyrite crystal (white) replaced along fractures by chalco-
pyrite (light gray) in a matrix of bornite. The chalcopyrite has formed as a reaction
product of the pyrite with the bornite depositing fluid, Magma Mine Superior, Arizona
(width of field = 2,000 μm). (*b*) Fractures in pyrite infilled by injected pyrrhotite with lit-
tle or no replacement, Great Gossan Lead, Virginia (width of field = 520 μm).

mal replacement, the secondary phase retains the same cation composition as the primary phase, with merely a change in oxidation state (e.g., hematite forming during oxidation of magnetite or violarite forming on pentlandite, Figures 7.34 and 9.8) or a change in anion (e.g., hematite replacing pyrite or anglesite replacing galena). Replacement may also selectively remove one cation while leaving another; this is frequently seen in the replacement of chalcopyrite or bornite by covellite (Figure 7.11a). The effects of the removal of cations during weathering are shown schematically for some common sulfides by the arrows in Figures 7.13 and 7.14. The removal of iron from hex agonal pyrrhotite results in an increase in the sulfur-to-metal ratio and the formation of monoclinic pyrrhotite (which often looks like "flames" along the margins of fractures) and ultimately in pyrite and marcasite (as grains, colloform masses, or "birds eyes"—see Figure 7.35). The iron removed from the pyrrhotite may leave the area in solution or may be precipitated as goethite along the fractures. The weathering of chalcopyrite or bornite usually results in the removal of iron before copper (i.e., so that the composition of the remaining sulfides moves in the direction of the arrow in Figure 7.14). Consequently, the outer margin of the chalcopyrite or bornite is converted to chalcocite, digenite, or covellite. The iron, as in the case of pyrrhotite weathering, is either removed or reprecipitated as goethite.

Selective removal of iron in preference to titanium is exhibited in the weathering of the iron-titanium oxides in placer ores. As shown in Figure 10.12, the selective removal of hematite laths from grains that contain intergrowths of hematite and ilmenite results in an increase in the titanium content of the remaining grain. This natural upgrading of the grains can significantly improve the quality and profitability of a placer ore deposit (see discussion in

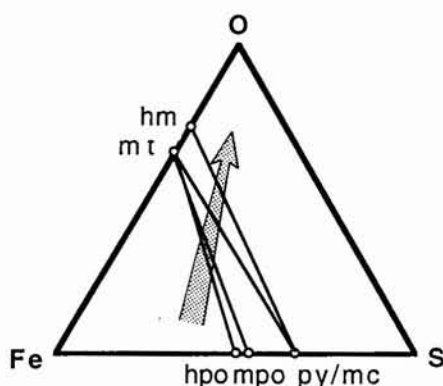**FIGURE 7.13** Weathering or oxidation of iron sulfides is shown schematically by the arrow on the Fe-S-O diagram. The addition of oxygen results in extraction of iron from the phases and the conversion of hexagonal pyrrhotite into monoclinic pyrrhotite and, ultimately, into pyrite or marcasite. The extracted iron may form an oxide or an hydroxide phase or may be removed from the system by fluids.
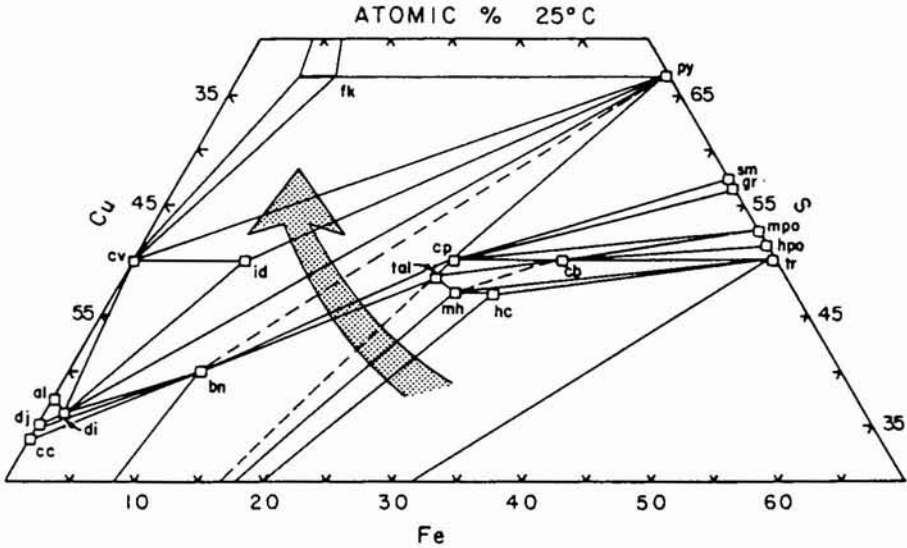
FIGURE 7.14 Weathering of the copper-iron sulfides is shown schematically by the arrow on the Cu-Fe-S system. During weathering, iron is preferentially removed from chalcopyrite (cp), forming bornite (bn) and, ultimately, digenite (di) and/or covellite (cv). Pyrite may form but is commonly absent because of the difficulty of nucleating pyrite at low temperatures.

Section 10.5). Chemical control of replacement is also demonstrated in Figure 7.12a, in which a copper-rich fluid has deposited bornite around earlier pyrite. Where the copper-bearing fluid encountered the pyrite and the chemical potential of FeS_2 was highest (e.g., within the centers of the fractured pyrite crystals), the replacement reaction resulted in the formation of chalcopyrite. Replacement may occur selectively, affecting only one phase in an intergrowth or particular zones in a compositionally zoned crystal (producing an *atoll structure*, see Figure 7.15). The reasons for such selective replacement may be extremely subtle and are, in most instances, poorly understood.

A final example of replacement is the open void "boxwork" texture composed of cellular crisscross laths of goethite, hematite, and sometimes pyrite, as are found in gossans (Figure 7.16).

FIGURE 7.15 Differing stages in the development of atoll structure resulting from the selective replacement of intergrown or compositionally zone crystals.

FIGURE 7.16   Boxwork texture of laths of hematite and goethite with residual pyrite in a gossan, Elba, Italy (width of field = 500 μm).

7.5 SECONDARY TEXTURES RESULTING FROM COOLING

Many ores form at elevated temperatures and have undergone cooling over temperature ranges that may be, for example, less than 100°C for many Pb-Zn ores in carbonates but as much as 1000°C for Fe-Ni-Cu ores in ultramafic rocks. As suggested by Figure 7.1, refractory minerals such as magnetite, chromite, pyrite, sphalerite, and some arsenides often retain their original composition and texture through the cooling episode, whereas many sulfides, sulfosalts, and native metals re-equilibrate compositionally and texturally during cooling. The textural effects resulting from cooling include those discussed below.

7.5.1 Recrystallization

Re-equilibration of ores on cooling is usually accompanied, to some degree, by recrystallization of the primary minerals, an effect that may or may not leave any vestige of the original texture. Thus, many massive chromite seams, which no doubt accumulated as well-formed octahedra settling from an igneous melt, have been modified by prolonged annealing, as discussed in Section 7.7.

7.5.2   Exsolution and Decomposition

Many ore minerals undergo compositional or structural adjustments in the form of exsolution or inversion as they cool from the temperatures of initial crystallization or the maximum temperature of metamorphic recrystallization. In exsolution, one phase is expelled from another, often in a characteristic pattern. A list of some commonly observed host and exsolved phases is given in Table 7.1; a more complete list is given by Ramdohr (1969, pp. 190–198).

The form of the exsolved phase varies with the minerals involved, their relative proportions, and the postdepositional cooling history of the ore. The exsolution process results from diffusion (usually of metal atoms through a sulfur or oxygen lattice), the nucleation of crystallites, and the growth of crystallites or crystals. Similarities of crystal structure and chemical bonding between host and exsolved phase, particularly the matching of atomic arrangements in specific layers resulting in a shared plane of atoms, frequently dictate that exsolution is crystallographically controlled (coherent exsolu-

TABLE 7.1   Examples of Ore Minerals Frequently Encountered in Exsolution Textures

| Host Phase	Exsolved Phase	Nature of Commonly Observed Intergrowth
Arsenic or antimony	Stibarsen	Myrmekitic
Bornite	Chalcopyrite	Basket weave
Bornite	Chalcocite-digenite	Roughly cubic network
Chalcopyrite	Cubanite	Sharply bounded laths
Chalcopyrite	Sphalerite	Stars, crosses
Chalcopyrite	Mackinawite	Lamellae, irregular wisps
Chalcopyrite	Bornite	Basket weave
Galena	Matildite	Lamellae
Hematite	Ilmenite	Lens-like lamellae
Ilmenite	Hematite	Lens-like lamellae
Kamacite	Plessite	Lamellae in triangular pattern
Magnetite	Ilmenite	Lamellae in triangular pattern
Magnetite	Ulvöspinel	Lamellae in triangular pattern
Pb-Sb and Pb-Bi sulfosalts	Pb-Sb and Pb-Bi sulfosalts	Lamellar
Pyrrhotite	Pentlandite	Lamellae or flames
Silver	Dyscrasite	Lamellae
Sphalerite[a]	Chalcopyrite	Rows of blebs
Sphalerite	Pyrrhotite	Rows of blebs
Sphalerite	Stannnite	Dispersed blebs
Stannite	Chalcopyrite	Lamellae in triangular pattern
Stibarsen	Arsenic or antimony	Myrmekitic

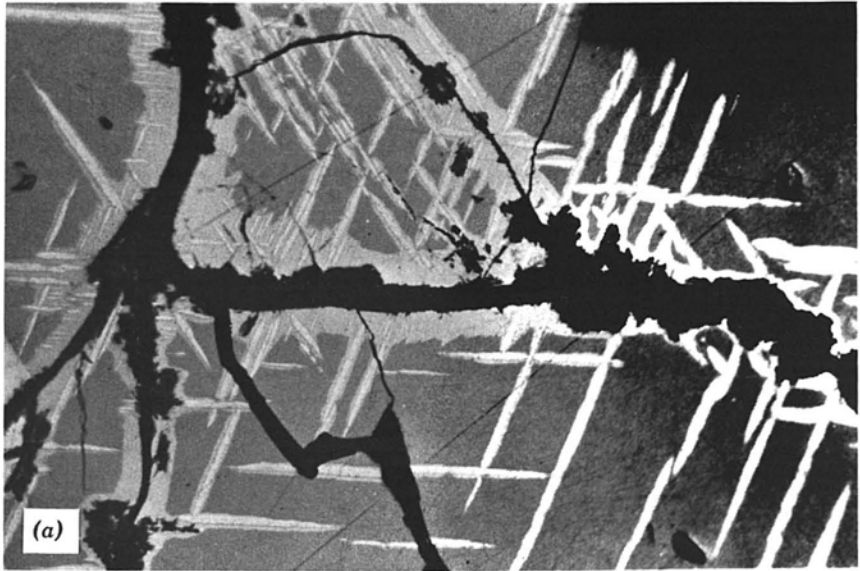[a]Usually not the result of exsolution; see text.
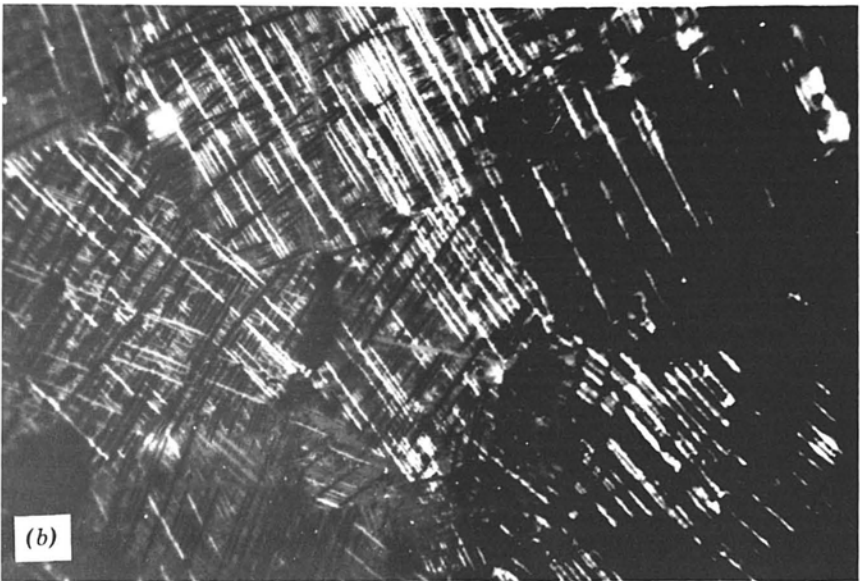
FIGURE 7.17 (*a*) Exsolution of chalcopyrite lamellae (light gray) within bornite (dark gray). Later alteration has resulted in the development of chalcocite (medium gray) along the edges of the fractures and as rims on the chalcopyrite lamellae, Grayson County, Virginia (width of field = 520 μm). (*b*) Fine lamellae of matildite (white and black) within a matrix of galena. This texture has resulted from the decomposition (on cooling) of an initially homogeneous phase; crossed polars, oil immersion; Leadville, Colorado (width of field = 265 μm). (*c*) "Allemontite," a myrmekitic texture of native
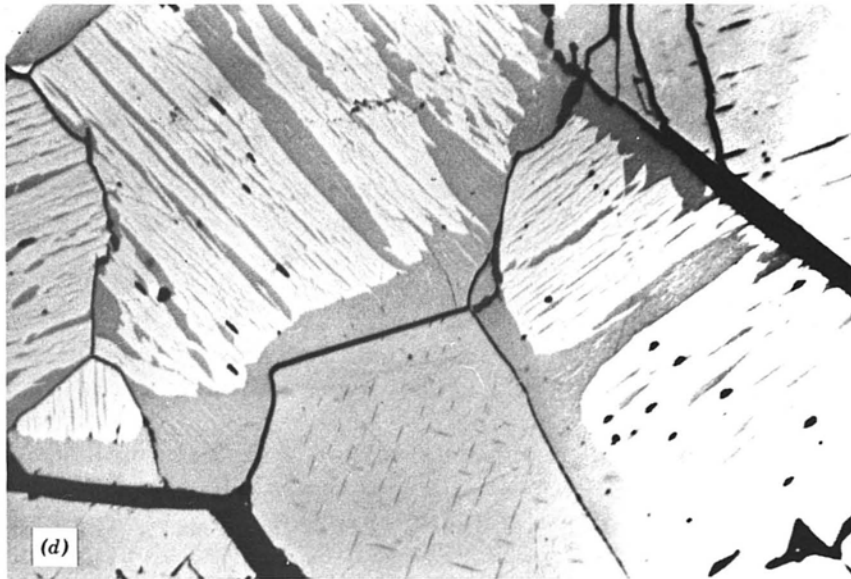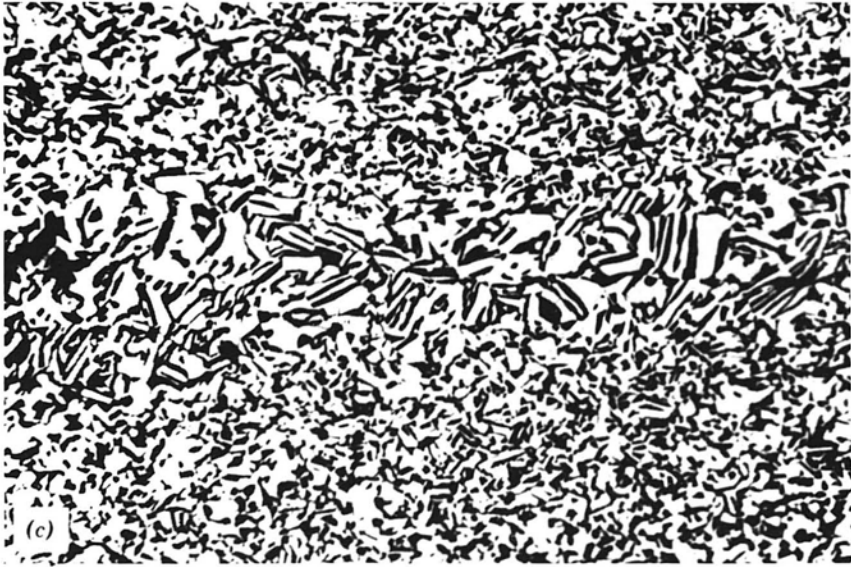
arsenic (black due to oxidation) and stibarson (white), which has resulted from the decomposition of an initially homogeneous phase (width of field = 520 μm). (*d*) Exsolution in coexisting FeTi oxides. Flanking grains of hematite-ilmenite solid solution have separated into hematite (white) and ilmenite (medium gray), and a central grain of Ti-magnetite has exsolved lamellae of ulvöspinel (width of field = 2,000 μm).

tion). For example, pentlandite exsolves such that the (111), (110), and (112) crystallographic planes are parallel to the (001), (110), and (100) planes, respectively, of the host pyrrhotite (Figure 8.8b), ulvöspinel exsolves parallel to the (111) planes of host magnetite (Figure 7.17d).

If parent and exsolved phases have completely different structures or if there is no crystallographic continuity across the interface between phases, noncoherent exsolution occurs. For example, it is apparent from phase equilibrium studies (Figure 8.18), that if pyrite and pyrrhotite equilibrate at elevated temperatures (~400°C or above), pyrite will exsolve on cooling. (See also Section 10.10 regarding the changes in pyrite and pyrrhotite during metamorphism.) However, the pyrite exhibits a considerable force of crystallization (i.e., a tendency to grow as euhedra at the expense of surrounding phases), which, when combined with the dissimilarity of the pyrite and pyrrhotite structures, results in the pyrite occurring as individual grains (commonly euhedral cubes) rather than as recognizable exsolution lamellae. The kinetics of the exsolution depend on temperature, degree of supersaturation, and the concentrations of impurities; in nature, virtually all pyrrhotites have compositions that have readjusted at low temperatures. A rigorous treatment of the kinetics and mechanisms of exsolution is beyond the scope of this text; for such detail, the reader is referred to the works of Yund and McCallister (1970), Putnis and McConnell (1980), or Kelly and Vaughan (1983). Decrease in the interfacial energy during exsolution is frequently accomplished by the exsolved phase taking on more equant forms. Hence, early formed flames of pentlandite in pyrrhotite coalesce into irregular veinlets, and well-defined thin lamellae of chalcopyrite in bornite (or vice versa) retain a basket weave texture but swell into bulbous lenses. A study of the exsolution textures observed in copper-iron sulfides (Brett, 1964) demonstrated that they are not particularly indicative of the rate of cooling or the temperature of initial formation of the ores.

The large variety of exsolution textures observed are difficult to classify using a simple terminology. However, certain terms are widely employed to describe the textures, notably *marginal, lamellar, emulsoid,* and *myrmekitic* exsolution textures (see Figure 7.17). The distinction between crystallographically controlled exsolution and similar replacement textures often can be made because intersecting lamellae show depletion at the junction in the former case and greater concentration in the latter case. Also, the depletion of exsolved material around a large bleb, known as *seriate distribution*, is a distinctive feature that is well illustrated in Figure 7.17d, which shows the exsolution intergrowths in FeTi oxides, among the most important and widely observed of such textures.

The exsolution of hematite and ilmenite (in widely varying proportions) results from cooling and is very commonly found in many types of high-grade metamorphic and igneous rocks. "Black sands," accumulated in many sedimentary environments (see Section 10.5), usually contain a large proportion of grains exhibiting hematite-ilmenite intergrowths.

An example of the confusion that can arise in the interpretation of ore textures is provided by sphalerite-chalcopyrite intergrowths. In many types of ores, sphalerite contains chalcopyrite in the form of randomly dispersed or crystallographically oriented rows of blebs and rods, each of which may be 1–20 μm across (Figure 7.18). This form of chalcopyrite, appropriately termed "chalcopyrite disease" by Barton and Bethke (1987), has commonly been ascribed to exsolution on the cooling of the ores after emplacement. The detailed work of these authors and the supporting evidence of experimental studies (Wiggins and Craig, 1980; Hutchison and Scott, 1981) have demonstrated, however, that chalcopyrite will not dissolve in sphalerite in significant amounts unless temperatures are above 500°C. These data, and the observation of chalcopyrite-bearing sphalerites in Zn-Pb ores in carbonates (which form at 100–150°C) and in unmetamorphosed volcanogenic ores (which form at 200–300°C) suggest that temperature-dependent exsolution is not the means by which these intergrowths form. Furthermore, detailed studies of doubly polished thin sections of these ores (Barton, 1978; Barton and Bethke, 1987; and Figure 3.2) reveal that some of the chalcopyrite is actually present at myrmekitic worm- or rod-like bodies that may extend up to several hundred microns. The most detailed study of these features, by Barton and Bethke
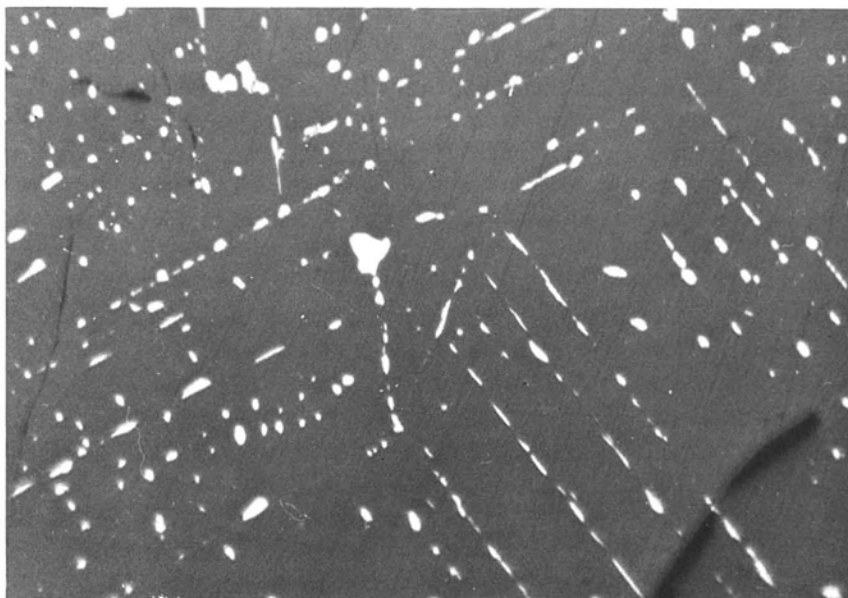

FIGURE 7.18 Grains and rods of chalcopyrite oriented within sphalerite. This assemblage often has been interpreted as the result of exsolution, but experimental studies reveal that sphalerite could not dissolve sufficient copper to form this texture by exsolution. See text for additional discussion. Great Gossan Lead, Virginia (width of field = 520 μm).

(1987), has concluded that the chalcopyrite results either by epitaxial growth during sphalerite formation or by replacement as copper-rich fluids react with the sphalerite after formation. During metamorphism, finely dispersed chalcopyrite may be redistributed when the sphalerite recrystallizes, so that it remains concentrated along the sphalerite grain boundaries.

Exsolution itself is a form of decomposition, because the original high-temperature composition no longer exists as a single homogeneous phase. However, the term "decomposition" is more commonly applied when a phase undergoes an abrupt change into two phases of distinctly different compositions, as in *eutectoidal breakdown*. The term "decomposition" is also applied to the breakdown of the central portion of a complete solid solution series, with the resulting development of an intimate intergrowth of compositionally distinct phases. Eutectoidal breakdown on cooling is well known in metallurgical studies, but relatively few mineral examples have been verified. Digenite, Cu_9S_5, is not stable below 70°C unless it contains ~1% iron and decomposes on cooling below this temperature to form a complex mixture of anilite and djurleite (see the Cu-S phase diagram in Figure 10.8). If the original composition before cooling is more Cu-rich, the decomposition may result in the formation of a mixture of chalcocite and djurleite. In a detailed study of the Cobalt-Gowganda, Ontario ores, Petruk (1971) has reported a complex intergrowth of galena and chalcocite that apparently has formed as a result of the decomposition of a Cu-Pb sulfide that is only stable at high temperature (Craig and Kullerud, 1968).

Two examples of textures resulting from the decomposition of the central portion of a solid solution series are lath-like matildite-galena intergrowths (Figure 7.17b) and the myrmekitic arsenic- (or antimony-) stibarsen intergrowths referred to as "allemontite" (Figure 7.17c). The fineness of the intergrowth (sometimes on a scale of a few microns) and the similarity in appearance of constituent phases can easily result in their misidentification as a single phase.

7.5.3 Inversion

Inversion of a mineral from one structural form to another of the same composition is not often easily discernible texturally but may produce characteristic twinning. Sometimes, even though inversion has occurred, the crystal morphology of the high-temperature phase is retained as a *paramorph*. Some high-temperature phases always invert so rapidly on cooling that only the low-temperature forms are observed (e.g., troilite, chalcocite, acanthite). Unfortunately, the twinning in acanthite, once thought to be diagnostic of inversion, can form below the inversion temperature of 176°C (Taylor, 1969). Certain other phases that are observed as both high- and low-temperature forms (e.g., cinnabar-metacinnabar; famatinite-luzonite) may not be diagnostic of formation conditions, because one of the forms is metastable.

Marcasite, although apparently never thermodynamically stable, commonly forms in low-temperature environments, including coals, black shales,

and carbonate- and sediment-hosted zinc-lead deposits. It is also frequently observed in supergene assemblages, especially forming along fractures in pyrrhotite. However, examination of the iron sulfides in these occurrences often reveals pyrite grains that exhibit the lath-like and radiating patterns typical of marcasite. Murowchick (1992) has pointed out that inversion of marcasite to pyrite results in a 2.6% volume reduction that leaves characteristic small pores. In contrast, the formation of marcasite or pyrite at the expense of pyrrhotite during weathering results in about a 30% volume reduction.

7.5.4   Oxidation-Exsolution and Reduction-Exsolution

Exsolution lamellae of ilmenite in magnetite (and less commonly of magnetite in ilmenite) are often present in a relative volume that exceeds the known solubility limits for these minerals. Lindsley (1976) has explained the mechanism by which these lamellae form with reference to the fO_2-T plot for the Fe-Ti oxides given in Figure 9.13. On this plot, the curves for magnetite-ulvöspinel solid solution (Mt-Usp) dip more steeply and those for hematite-ilmenite solid solution (Hem-Ilm) dip less steeply than the curves for buffers such as Ni-NiO, fayalite-magnetite-quartz or most fluids. Consequently, on cooling along a buffer curve or in the presence of a fluid of constant composition, a given Mt-Usp will undergo oxidation and lamellae of ilmenite will form on the (111) planes. Conversely, a Fe_2O_3-rich ilmenite, cooled under similar conditions, will be reduced, yielding lamellae of Ti-magnetite parallel to the (0001) planes.

7.5.5   Thermal Stress

Most ore minerals have approximately the same coefficients of thermal expansion, and thus most mono or polymineralic masses suffer little induced strain on cooling. One significant exception is pentlandite, $(Fe,Ni)_9S_8$, which has a coefficient of thermal expansion that is 2–10 times larger than such sulfides as pyrrhotite and pyrite with which it is generally associated (Rajamani and Prewitt, 1975). As a result, the chain-like veinlets of pentlandite (Figure 9.5) that form at elevated temperatures (300–600°C) by coalescence of early exsolved lamellae, are typically fractured, because they have undergone much greater shrinkage than the host pyrrhotite.

7.6   SECONDARY TEXTURES RESULTING FROM DEFORMATION

Many ores contain textural evidence of deformation. The evidence ranges from minor pressure-induced twinning to complete cataclasis. The degree to which individual mineral grains both respond to and preserve deformational effects ranges widely, depending on the mineral, the rate of strain, the nature of the deformation, the associated minerals, the temperature at the time of deformation, and the postdeformational history. The response threshold of min-

erals appears to be primarily a function of hardness. Hence, minerals such as many native metals, sulfosalts, and copper and silver sulfides deform most readily; copper-iron sulfides and monosulfides, less readily; and disulfides, oxides, and arsenides, least readily. Accordingly, in polymineralic ores, deformation textures are often evident in only some minerals. The softer minerals deform most readily, but they also recrystallize most readily, so that the deformational effects are obliterated before those in more refractory minerals. Specific deformation features commonly observed include those discussed in the following subsection.

7.6.1 Twinning, Kinkbanding, Pressure Lamellae

Twinning, kinkbanding, and pressure lamellae occur in ores subjected to any degree of deformation and can even be artificially introduced into some of the softer minerals by rough treatment of specimens. Twinning may occur in minerals during initial growth, during structural inversion on cooling (Section 7.5), or as a result of deformation. Although little or no quantitative study has ever been undertaken, Ramdohr (1969) suggests that the three major types of twinning (illustrated in Figures 7.19 and 7.20) can be distinguished as follows:

Growth	Occurs as lamellar twins of irregular width that are unevenly distributed, present in only some grains, and may be strongly interwoven
Inversion	Commonly occurs as spindle-shaped and intergrown networks not parallel throughout grains
Deformation	Occurs as uniformly thick lamellae, commonly associated with bending, cataclasis, and incipient recrystallization (regions of very small equant grains), with lamellae often passing through adjacent grains

These criteria are useful but not infallible guides to the identification of major types. Clark and Kelly (1973), in investigating the strength of some common sulfide minerals as a function of temperature, show that deformation in pyrrhotite may be as kinkbanding (Figure 7.20c), kinked, or bent subparallel lamellae, each of which show undulose extinction, or twinning. At less than 2 Kbar, kinkband deformation predominates below ~300°C, whereas above this temperature both kinking and twinning are common. Pyrrhotite and many other sulfides that are only moderately hard (e.g., stibnite, bismuthinite) also commonly contain "pressure lamellae" (Figure 7.21), slightly offset portions of grains that exhibit either undulatory extinction or slightly different extinction positions. Pressure-induced twins and pressure lamellae (Figure 7.20a and Figure 7.20d) often terminate in regions of brittle fracture and crumpling, or very fine-grained regions in which crushed grains have recrystallized.
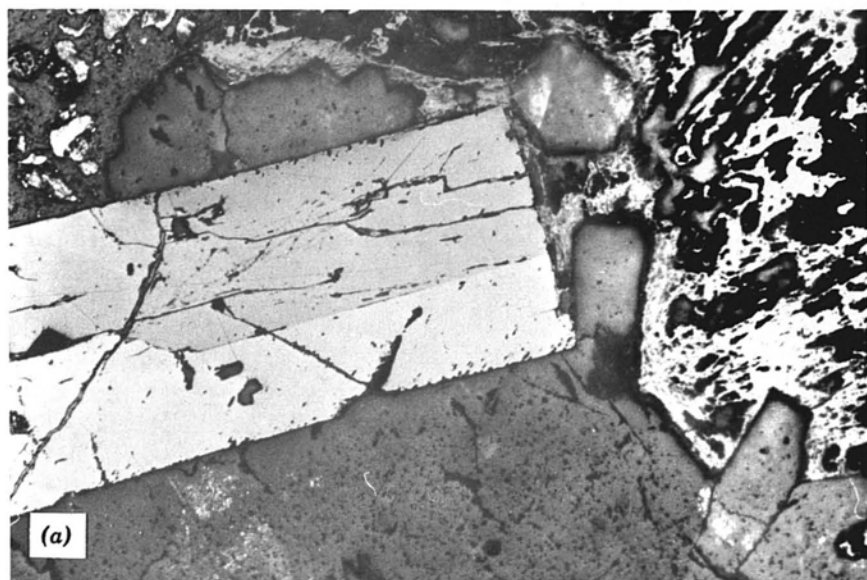
FIGURE 7.19   (*a*) Growth twin of wolframite. (*b*) Polysynthetic twinning developed in synthetic acanthite that has inverted from argentite on cooling from initial formation at 400°C; crossed polars, oil immersion (width of field = 190 μm).

Breaking of specimens by hammering or damage caused during grinding or even in careless polishing can induce local pressure twinning in some very soft phases, such as native bismuth (Figure 7.20b), argentite, and molybdenite. The cause of such twinning is usually recognizable because of its local dis-
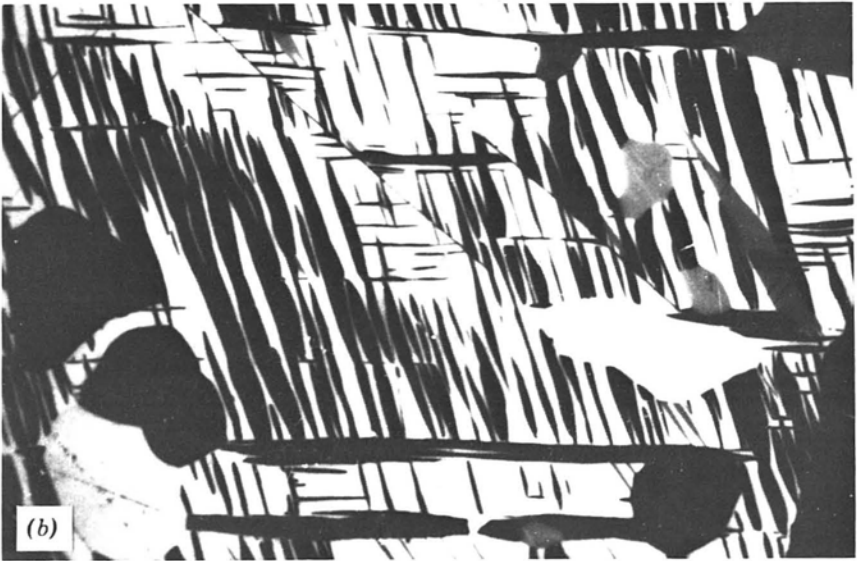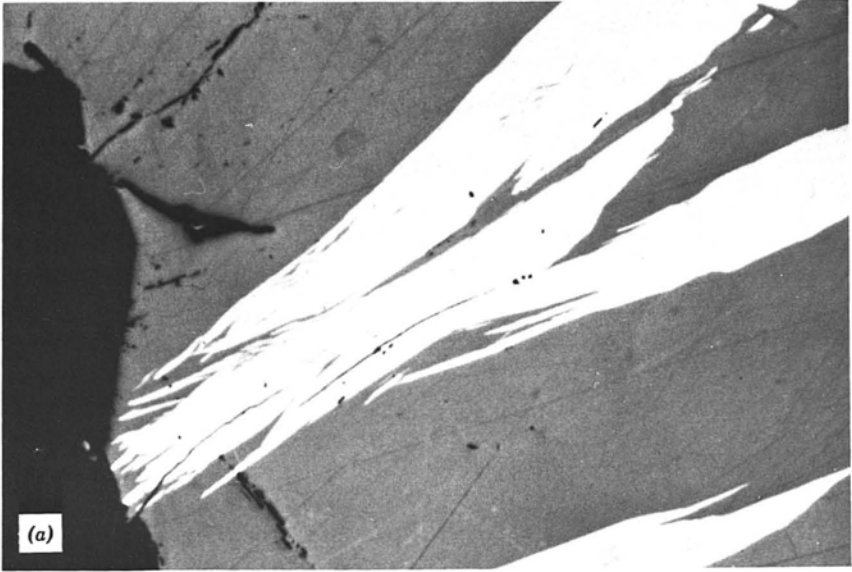
FIGURE 7.20   (a) Deformation twins in pyrrhotite, Great Gossan Lead, Virginia; crossed polars (width of field = 520 μm). (b) Polysynthetic twinning developed in native bismuth as a result of deformation, Nipissing Mine, Cobalt, Ontario; crossed polars, oil immersion (width of field = 210 μm). (c) Kinkbanding in pyrrhotite accentuated by thin layers of micas, Cherokee Mine, Ducktown, Tennessee (partially crossed nicols; width of field = 0.24 mm). (d) Deformation twinning induced in specular hematite, Rana Gruber, Norway (width of field = 1,200 μm).
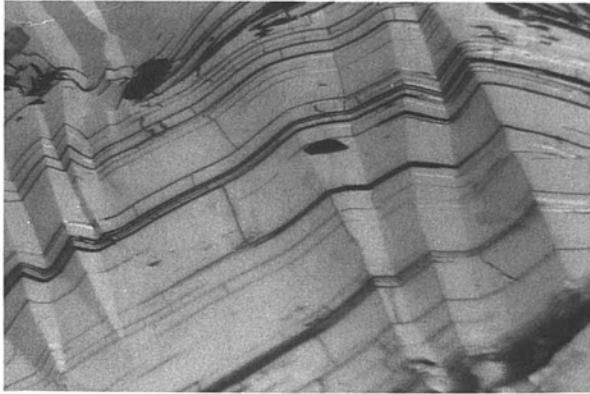
(c)
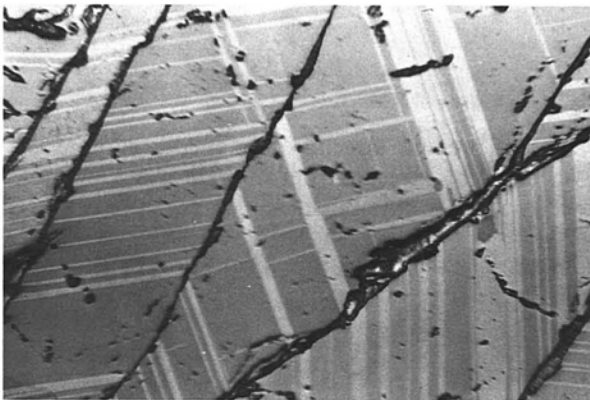
(d)

FIGURE 7.20   (*Continued*)

tribution or association with scratches; it can often be induced in native bismuth by merely drawing a needle point across a polished surface.

7.6.2   Curvature or Offset of Linear Features

Deformation of ores is often evidenced by the curvature or offset of normally linear or planar features, such as crystal faces, cleavages, fractures, twins, exsolution lamellae, and primary mineral layering or veining. The triangular cleavage pits in galena, so diagnostic in identification, commonly serve as a measure of deformation. Although the boundary of a single pit may exhibit curvature, the effects are most often seen in the curvature of a row of such cleavage pits (Figure 7.22). Deformation-induced twin lamellae in pyrrhotite, ilmenite, chalcopyrite, and many other minerals frequently exhibit significant curvature and commonly extend across several grains, whereas growth or inversion twins are usually confined within individual grains.

FIGURE 7.21 Complex pressure lamellae developed in stibnite as a result of deformation; the wide variety of colors results from different crystallographic orientations of the lamellae; crossed polars (width of field = 520 μm).
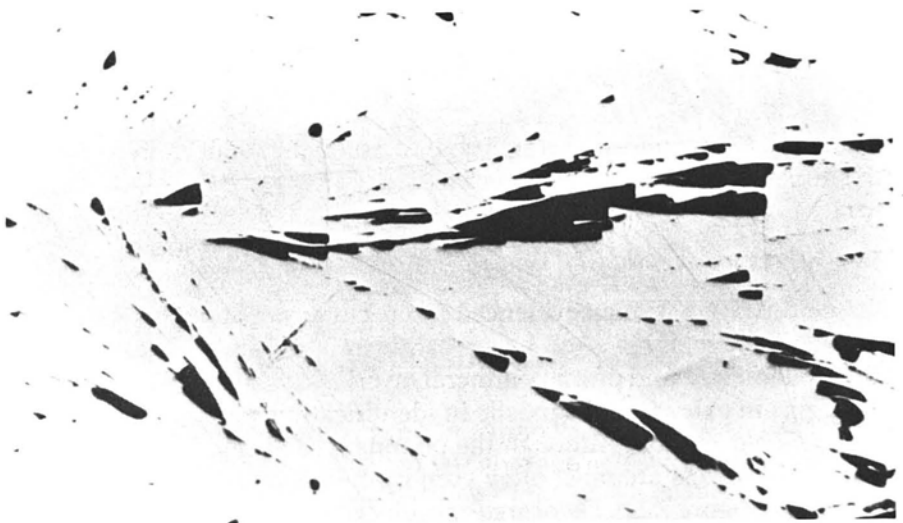

FIGURE 7.22 Curved cleavage pits that have developed in galena as a result of postdepositional deformation, Austinville, Virginia (width of field = 520 μm).

Exsolution intergrowths of cubanite in chalcopyrite, ilmenite in hematite (or vice versa), chalcopyrite in sphalerite, pentlandite in pyrrhotite, and bornite in chalcopyrite (or vice versa) are often linear (or planar) features that are crystallographically controlled. Curvature of the laths, rows of blebs, flames, or rods is indicative of deformation; however, it is not always clear whether the exsolution or the deformation occurred first.

Folding or offseting of primary mineral banding is a common feature in many deformed ores on both micro- and macroscales. Folding often results in a relatively ductile flow of such softer sulfides as chalcopyrite, galena, and pyrrhotite but brittle fracture of such harder minerals as pyrite, arsenopyrite, and magnetite. Thus, the softer sulfides infill fractures between discontinuous broken portions of harder mineral zones (Figure 10.27). Microscale offsetting of mineral bands or mineralized veins (Figure 8.4a), commonly with infilling by later generations of ore or gangue minerals, is frequently seen in ores.

7.6.3 Schlieren

Deformed ores often contain zones along which shearing has occurred. In such zones, known as *schlieren*, the ore minerals may be pulverized and smeared out parallel to the direction of movement The schlieren are usually planar features in which the ore minerals are very fine grained (sometimes recrystallized) relative to the surrounding rock; typically, equant minerals such as galena are frequently present as elongate (often strained and fractured) grains.

7.6.4 Brecciation, Cataclasis, and Durchbewegung

Deformation in ores is often evidenced by fracturing or brecciation of ore and gangue minerals, especially (but not exclusively) of those that are harder and more brittle, such as pyrite, chromite, and magnetite. The amount of brecciation depends on both the degree of deformation and the mineralogy of the ore. Thus, moderate deformation will result in considerable brecciation of massive pyrite, magnetite, or chromite ore where all strain is relieved by brittle fracture of these minerals. In contrast, pyrite admixed with pyrrhotite or chalcopyrite usually suffers little, even under extreme deformation, because the strain is taken up in the softer sulfides. A notable exception to this is the "rolled" pyrite from Sulitjelma, Norway. In this ore, the pyrite cubes have been markedly rounded by being "rolled" in the matrix pyrrhotite and chalcopyrite during severe deformation. Local brecciation of pyrite also occurs where pyrite grains, otherwise protected by the host pyrrhotite, impinge upon one another (Figure 7.23). Minor brecciation grades into complex cataclasis with an increasing degree of fragmentation and disorientation, eventually involving both ore and gangue minerals (Figure 7.24); this penetrative deformation has been termed *durchbewegung* (literally "move through") by Vokes (1969). In fault zones and in ores that have suffered penetrative high-grade meta-
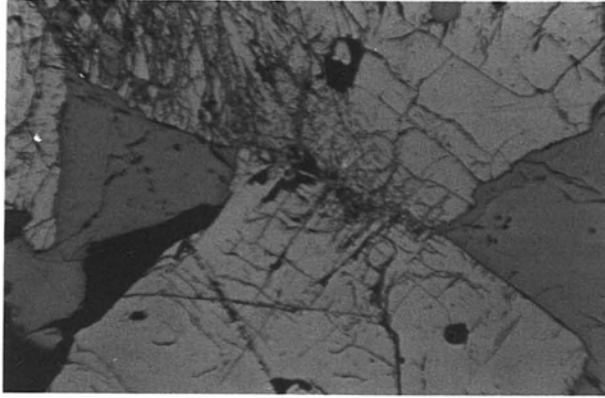
FIGURE 7.23   Despite intense deformation, much of the pyrite in the pyrite-pyrtho-tite ores of Ducktown, Tennessee, show no fracturing, because the softer interstitial pyrrhotite has deformed. Here, however, pyrite grains show localized fracturing, because they have impinged upon one another (width of field = 1,200 µm).

morphism, there may be pulverization of ore and gangue minerals, complete randomness of fragment orientation, the development of "ball textures," in which fragments of foliated gangue are rounded into "balls," and extensive development of the deformational features previously described. Injection of
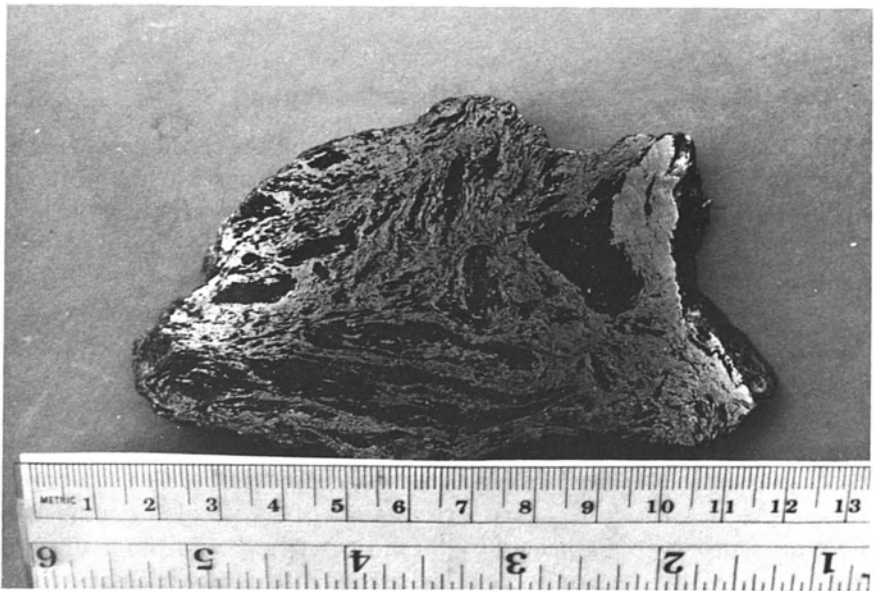

FIGURE 7.24   Durchbewegung texture developed in intensely deformed pyrrhotite. The black silicate inclusions were stretched and rotated as the pyrrhotite matrix flowed under pressure, Great Gossan Lead, Virginia. The scales are in centimeters and inches.

softer ore minerals into fractures and cleavages in more brittle ore minerals and gangue minerals is common (Figure 10.27).

7.7 SECONDARY TEXTURES RESULTING FROM ANNEALING AND METAMORPHIC CRYSTAL GROWTH

After initial formation, many ores have been subjected to slow cooling or have passed one or more times through metamorphic cycles in which they were subjected to prolonged periods of slow heating and slow cooling. The textural effects of this treatment may be indiscernible, or may lead to distinctive annealed grain boundaries or even to the growth of porphyroblastic crystals.

7.7.1 Annealing

The annealing effects of the slow cooling of ores after deposition or slow heating during metamorphism can significantly alter the original textures. Since both cooling and metamorphism are prolonged annealing processes, the effects discussed here may produce similar textures to those discussed in Section 7.2. The most characteristic feature of annealing is recrystallization to minimize the areas of grain surfaces and interfacial tension through the development of roughly equant grains with 120° interfacial (or *dihedral*) angles (Figure 7.25). The interfacial angles observed at triple junctions of annealed monomineralic aggregates tend toward 120°, whereas those of polymineralic aggregates vary as a function of the mineralogy. The interfacial angles of some equilibrated pairs of common sulfide minerals include galena-sphalerite (103° and 134°), chalcopyrite-sphalerite (106–108°), and pyrrhotite-
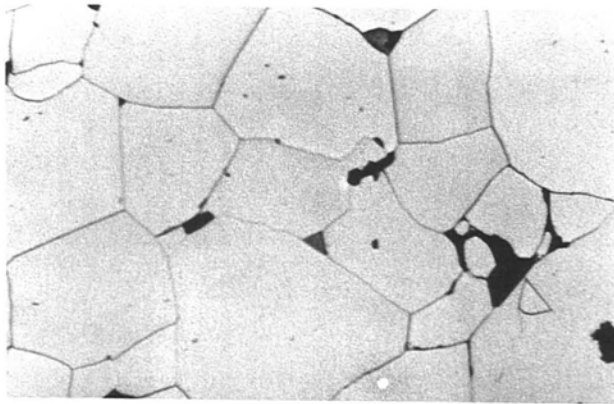

FIGURE 7.25 Annealed texture of recrystallized monomineralic pyrite sample. Note the common development of near 120° triple junctions, Mineral District, Virginia (width of field = 520 μm).

sphalerite (107–108°) (Stanton, 1972). Since the surface of the polished section, cut at random through the polycrystalline mineral aggregate, yields only apparent angles that can range from 0° to 180°, it is necessary to measure many interfacial angles in a given section in order to determine statistically the true angle. If a large number of angles are measured, the one most frequently observed will represent the true angle. During the annealing process, small grains are resorbed at the expense of larger ones; however, small grains of minor phases may remain trapped as lens-like bodies along the grain boundaries of larger grains (Figure 10.27d).

The re-equilibration that results from annealing can produce either zoned overgrowths on grains or the homogenization of grains containing primary growth zoning. For example, pyrite overgrowths on primary pyrite or the remains of primary growth zoning may be visible in normal polished sections but often require etching to become evident (Figure 2.10). Residual primary growth zoning in sphalerite or tetrahedrite is rarely evident in polished sections but can be observed in transmitted light using doubly polished thin sections (Figure 2.9).

7.7.2 Metamorphic Crystal Growth

Recrystallization during annealing, especially during metamorphism, usually results in an increase in grain size and may also result in the growth of
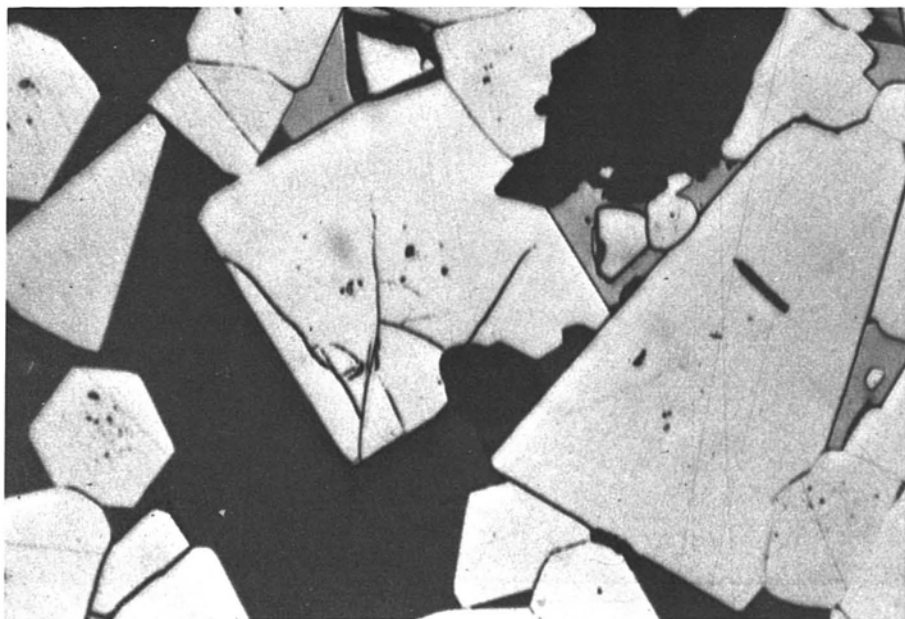

FIGURE 7.26   Annealed texture of recrystallized pyrite euhedra (light gray) within a matrix of sphalerite (dark gray), and minor chalcopyrite (medium gray). Mineral District, Virginia (width of field = 520 μm).

euhedral, sometimes porphyroblastic crystals, of such phases as pyrite (Figure 7.26), arsenopyrite, magnetite, and hematite. The growth of these minerals, like the well-known examples among metamorphic gangue minerals (e.g., garnet and staurolite), depends on the conditions of annealing and the bulk composition of the mineralized zone. Though commonly only a few millimeters in diameter, porphyroblasts may exceed 25 cm across, as observed in the pyrite-pyrrhotite ores of Ducktown, Tennessee (Figure 7.27). Porphyroblastic growth or overgrowth complicates paragenetic interpretation, because there may be no unequivocal means of distinguishing porphyroblasts from early formed euhedral crystals. Frequently, however, porphyroblasts contain different amounts and types of inclusions compared to the corresponding primary minerals in the ore. Furthermore, the types of inclusions may be indicative of the timing of crystal growth. Hence, the inclusion of high-grade metamorphic minerals (e.g., amphiboles, garnets, etc.) indicates that overgrowth occurred after metamorphism had reached a grade sufficient to form those metamorphic minerals.

Detailed studies of the large, generally euhedral pyrite crystals of the Ducktown, Tennessee, ores (Brooker, Craig, and Rimstidt, 1987; Craig, Vokes, and Simpson, 1991; Craig and Vokes, 1993) have revealed two principal types of inclusion patterns. The most common type is that of concentrically arranged inclusions of silicates (usually quartz, amphiboles, and carbonates) and sulfides (usually sphalerite, pyrrhotite, and chalcopyrite; see Figure 7.28). Such a pattern may indicate concentric growth outward in all directions from a central point, or it may indicate "snowball-type" growth that has been cut parallel to the axis of rotation. The other type of growth pattern is that of a spiral (Figure 7.29), much like that observed in rotated garnets. Both types of inclusion patterns may represent "snowball" growth, in which the difference in appearance results from the orientation of the cut. Hence, cutting a snowball-
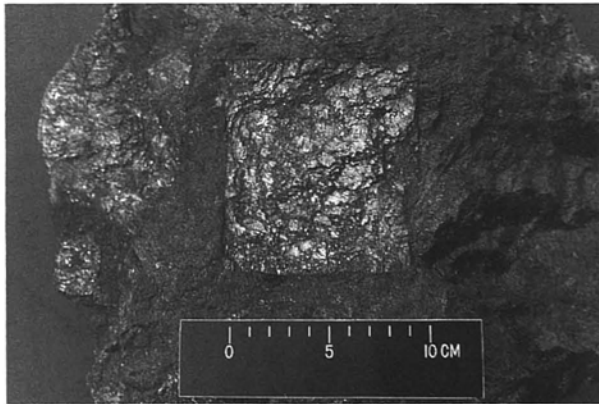

FIGURE 7.27   Ten-cm pyrite cube in the amphibolite grade regionally metamorphosed ores of the Ducktown, Tennessee, deposits.
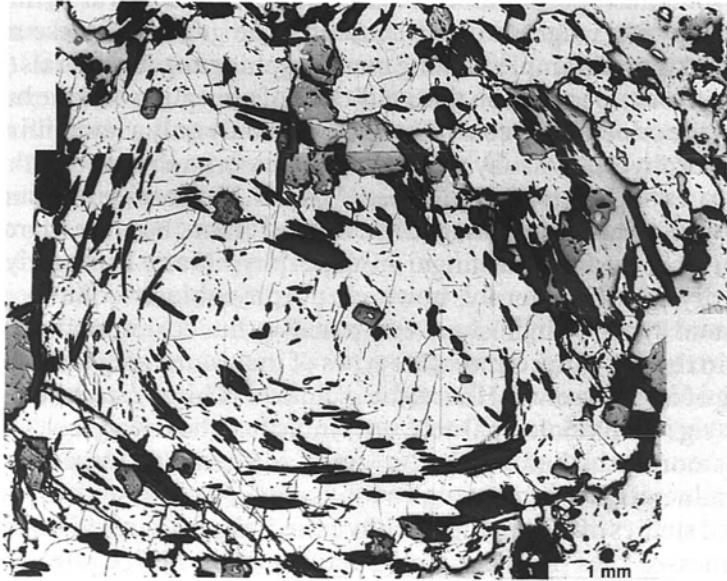
FIGURE 7.28 Five-mm pyrite crystal displaying a concentric pattern of amphibole inclusions incorporated during growth; gray phase is pyrrhotite. This is a composite image made up of 16 photomicrographs, Cherokee Mine, Ducktown, Tennessee.
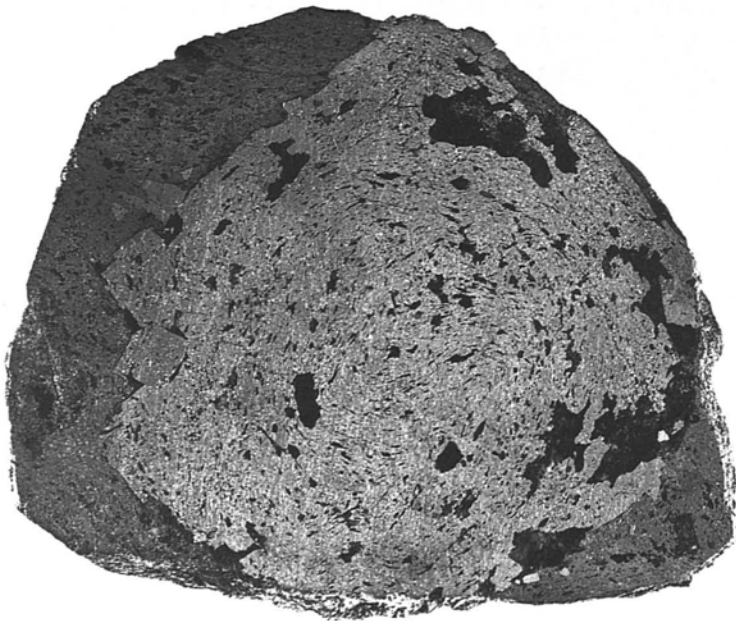

FIGURE 7.29 Ten-cm, equant, pyrite crystal, which exhibits a double-spiral inclusion pattern indicative of pyrite rotation of 360° relative to the enclosing pyrrhotite during growth, Cherokee Mine, Ducktown, Tennessee. (Reproduced from Craig et al, 1991, *Econ. Geol.* **86**, 1743; with permission.)

type grain perpendicular to its axis of rotation presents a spiral pattern instead of a concentric pattern. This relationship is illustrated in Figure 7.30.

The absolute amounts of the ore minerals probably change very little during most metamorphic episodes, despite significant changes in grain sizes and shapes. Exceptions to this would occur if there were significant oxidation or reduction reactions or if there were significant solubility of one phase in another as a function of temperature or pressure. Hence, the proportions of pyrite to pyrrhotite may change during a metamorphic cycle, and the proportions of pyrrhotite to sphalerite (and the sphalerite composition in terms of FeS content) may change as a function of pressure. (See Section 10.10 for an additional discussion of these points.)

7.8   TEXTURES OF PLACER GRAINS

Placer deposits are composed of the grains of ore minerals that have been weathered out of pre-existing rocks. Consequently, the mineral grains generally contain internal textures that reflect their initial origins but marginal and external textures that reflect the abrasion and weathering to which they have been subjected. Although nearly any ore mineral could, under some circumstances, be liberated from its host rock or ore and thus appear in a placer deposit, only a few actually occur with any frequency (see Section 10.5). Few sulfide minerals survive weathering without being completely oxidized. One notable exception appears to be the rounded pyrite grains in Precambrian conglomeratic deposits (see Section 10.6), which escaped oxidation apparently because of the lack of oxygen in the early atmosphere. In contrast, the oxide minerals cassiterite (SnO_2), ilmenite ($FeTiO_3$), rutile (TiO_2), and mag-
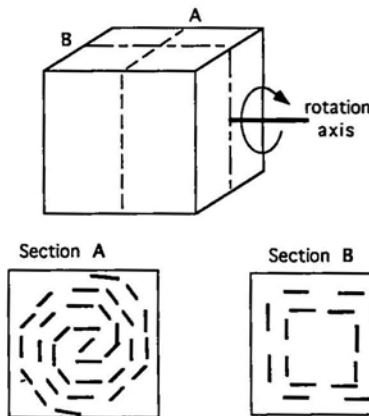

FIGURE 7.30   Schematic representation of how the inclusion patterns would appear in sections cut across (A) and parallel to (B), the rotation axis in a crystal that rotated as it grew.

netite (Fe_3O_4), and native gold (Au to AuAg) generally survive weathering quite well. Despite the varied original sources of these minerals, there are only a relatively few textures that are commonly encountered.

The weathering and erosional processes rapidly round and smooth the exterior surfaces of most placer grains, as is apparent in Figure 7.31. Other frequently observed marginal effects include the conversion of rutile grains into leucoxene around their margins, the oxidation of magnetite grains to hematite or goethite, especially along cleavage planes (Figure 7.34). This leads to the formation of "martite."

Ilmenite is particularly resistant to weathering and is the most abundant heavy mineral in many areas. It may display a wide variety of textures in placer grains, ranging from single crystals to polycrystalline aggregates. Commonly, ilmenite grains contain variable quantities of hematite as oriented lamellae, as shown in Figure 10.12. During weathering and erosion, selective dissolution of the more soluble hematite proceeds from the margins of the grains inward. The result, as shown in Figure 7.32, is that many ilmenite grains are left with hematite dissolved from around the edges or with only oriented holes where the hematite lenses used to be.

Placer gold grains (many are actually electrum in which the silver content exceeds 20 wt %) may possess a wide variety of initial shapes as the grains are liberated during weathering. Because of the softness and malleability of the gold, the grains readily undergo mechanical deformation that results in rounded to flattened nuggets. Although they have been long considered as relatively homogeneous materials that might include some fragments of original host or inherited detrital material, it is now widely recognized that many, if not most, placer gold grains develop rims of very high purity gold (Figure 7.33). The mechanisms by which these rims form are not completely understood, but they may occur as small localized patches or as complete surrounding layers.
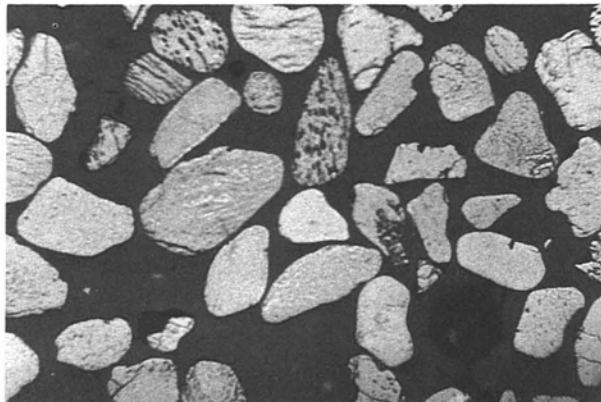

FIGURE 7.31   Placer ilmenite and rutile grains in a heavy mineral concentrate from Green Cove Springs, Florida, display a typical rounded to elongated shape (width of field = 1,200 μm).
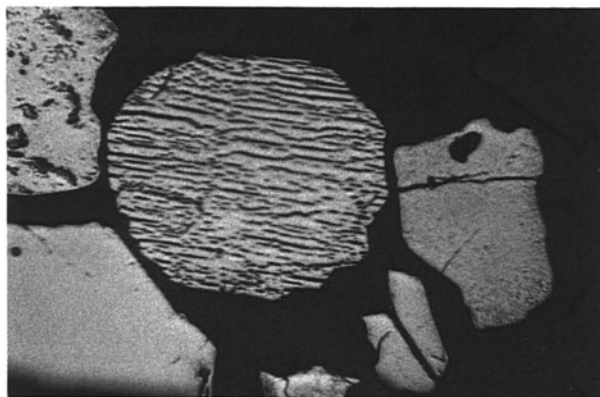
FIGURE 7.32   Placer ilmenite grains. The grains on the lower left and on the right are entirely ilmenite. The round central grain, originally an ilmenite with hematite lamellae (see Figures 7.17d and 9.11), has had all of the hematite dissolved out during weathering, Lilesville, North Carolina (width of field = 600 µm). Compare also with Figure 10.12.

The thicknesses range from less than 1 µm to more than 100 µm, but their boundaries with the underlying core gold or electrum are always very sharp. Because the rims are usually of very high fineness (usually more than 95% gold), they are a more deep yellow color than the lower fineness interiors; this is easily seen especially by use of oil immersion. Gentle etching with dilute cyanide solutions can enhance the appearance of these rims.
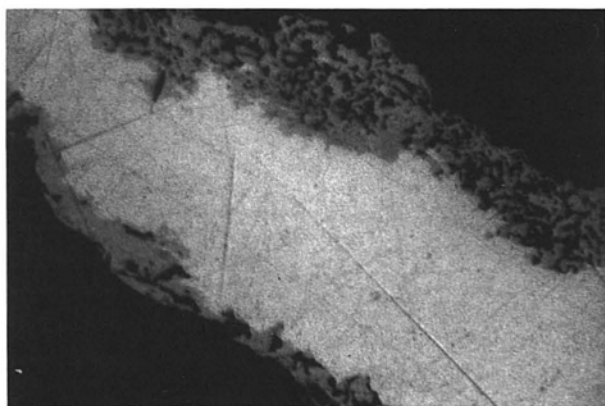

FIGURE 7.33   Placer electrum grain with a well-developed and sharply bounded rim (darker) of high-purity gold. Such rims, which may be very delicate or more solid (see Figure 10.14), are common on placer gold grains; Lilesville, North Carolina (width of field = 600 µm).
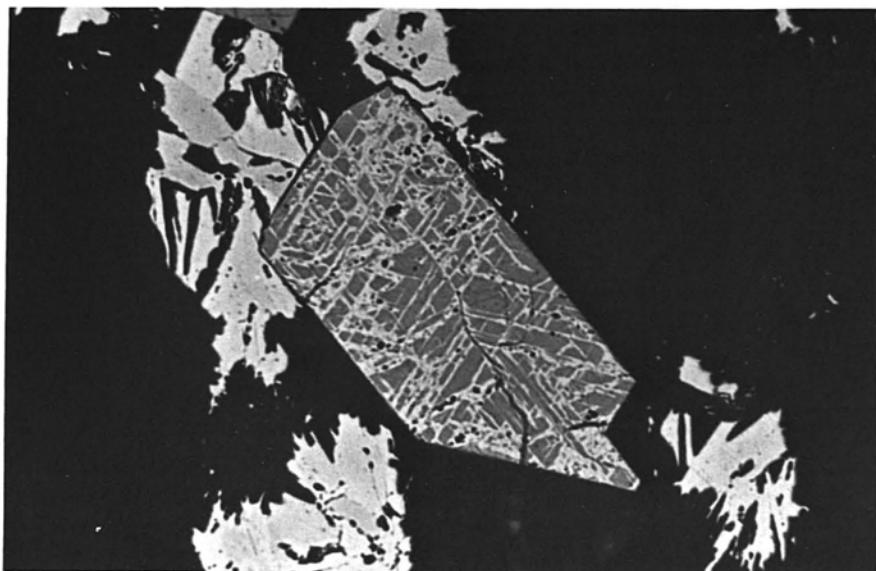
FIGURE 7.34 "Martite" in which hematite (white) has developed along crystal-lographically preferred planes in magnetite as a result of oxidation (width of field = 240 μm).

7.9 SPECIAL TEXTURES

A number of the textures observed in ore minerals are sufficiently distinctive or widely observed to have been given special names. Amongst primary depositional textures are *framboids* (Figure 10.5b), the aggregates of spherical
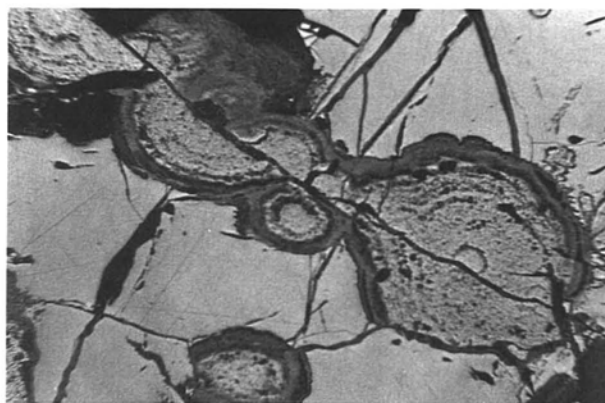

FIGURE 7.35   Well-developed "bird's-eye" texture composed of pyrite and marcasite, formed along a fracture during weathering of pyrrhotite, Great Gossan Lead, Virginia (width of field = 1,200 μm).
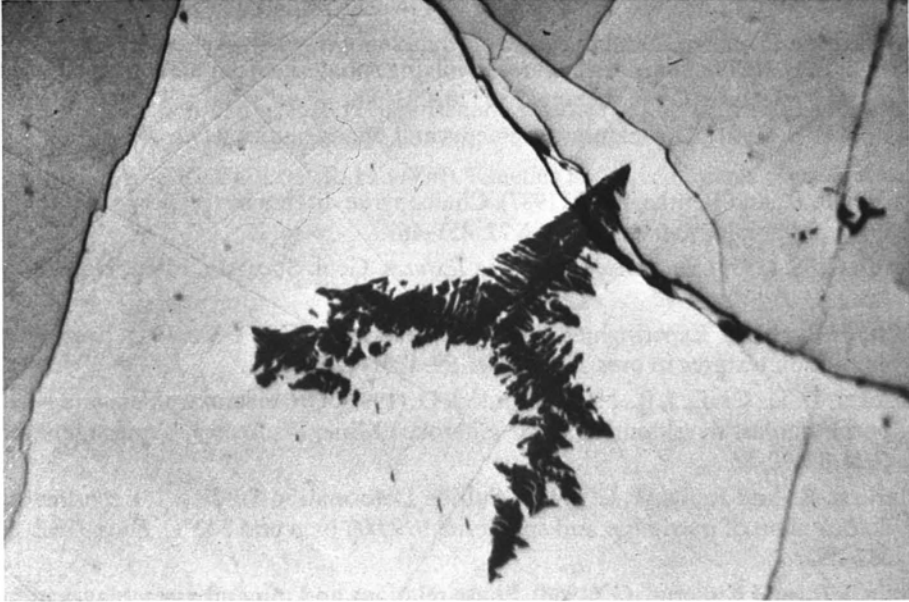
FIGURE 7.36   Sphalerite "star" in chalcopyrite, Mineral District, Virginia (width of field = 330 μm).

particles often seen in pyrite and in uraninite. Similar to these primary textures are the *oolitic* textures familiar from carbonate rocks but also found in iron and manganese ores (see Section 10.2). Among replacement textures, the replacement of magnetite by hematite along cleavage (111) directions is termed *martitization* (Figure 7.34), and the characteristic alteration of pyrrhotite to a fine mixture of pyrite and marcasite results in *birds eye* texture (Figure 7.35). Some exsolution textures are particularly characteristic, such as the *flames* of pentlandite in pyrrhotite (Figure 8.8b) and the *stars* of exsolved sphalerite found in some chalcopyrite (Figure 7.36).

7.10   CONCLUDING STATEMENT

Rarely does a single texture provide unequivocal evidence regarding the origin or history of an ore deposit. Commonly, a variety of textures representing different episodes in the development and subsequent history of a deposit are observed. This chapter has not provided an exhaustive discussion of the great variety of textures seen in ores, but it has introduced some of the most commonly encountered types. With careful observation, common sense, and a little imaginative interpretation that incorporates whatever is known of the geological setting of a deposit, much can be learned about the origin and postdepositional history of an ore from the study of ore textures.

REFERENCES

Barton, P. B. (1978). Some ore textures involving sphalerite from the Furutobe Mine, Akita Prefecture, Japan. *Mining Geol.* **28**, 293–300.

Barton, P. B. (1991). Ore textures: problems and opportunities. *Mineral Mag.* **55**, 303–315.

Barton, P. B., and Bethke, P. M. (1987). Chalcopyrite disease in sphalerite: pathology and epidemiology. *Amer. Mineral.* **72**, 451–467.

Bastin, E. S. (1959). *Interpretation of Ore Textures.* Geol. Soc. Am. Mem. No. 45, 101 pp.

Brett, P. R. (1964). Experimental data from the system Cu-Fe-S and its bearing on exsolution textures in ores. *Econ. Geol.* **59**, 1241–1269.

Brooker, D. D., Craig, J. R., and Rimstidt, J. D. (1987). Ore metamorphism and pyrite porphyroblast development at the Cherokee Mine, Ducktown, Tennessee. *Econ. Geol.* **82**, 72–86.

Clark, B. R., and Kelly, W. C. (1973). Sulfide Deformation Studies: I. Experimental deformation of pyrrhotite and sphalerite to 2,000 bars and 500°C. *Econ. Geol.* **68**, 332–352.

Craig, J. R., and Kullerud, G. (1968). Phase relations and mineral assemblages in the copper-lead-sulfur system. *Am. Mineral.* **53**, 145–161.

Craig, J. R., and Vokes, F. M. (1993). The metamorphism of pyrite and pyritic ores; an overview. *Mineral. Mag.* **57**, 3–18.

Craig, J. R., Vokes, F. M., and Simpson, C. (1991). Rotational fabrics in pyrite from Ducktown, Tennessee. *Econ. Geol.* **86**, 1737–1746.

Edwards, A. B. (1947). *Textures of the Ore Minerals.* Australian Institute of Mining and Metallurgy, Melbourne, Australia.

Hutchison, M. N., and Scott, S. D. (1981). Sphalerite geobarometry in the system Cu-Fe-Zn-S, *Econ. Geol.* **76**, 143–153.

Kelly, D. P., and Vaughan, D. J. (1983). Pyrrhotite-pentlandite ore textures: a mechanistic approach. *Mineral Mag.* **47**, 453–463.

Lindsley, D. H. (1976). Experimental studies of oxide minerals. In D. Rumble (ed.), *Oxide Minerals.* Mineral. Soc. Am. Short Course Notes 3, L61–L88. Washington, D.C.

Murowchick, J. B. (1992). Marcasite inversion and the petrographic determination of pyrite ancestry *Econ. Geol.* **87**, 1141–1152.

Petruk, W., and Staff (1971). Characteristics of the Sulphides. In The silver-arsenide deposits of the Cobalt-Gowganda Region, *Ontario. Can. Mineral* **11**, 196–221.

Putnis, A., and McConnell, J. D. C. (1980). *Principles of Mineral Behavior.* Elsevier, New York.

Rajamani, V., and Prewitt, C. T. (1975). Thermal expansion of the pentlandite structure. *Am. Mineral.* **60**, 39–48.

Ramdohr, P. (1969). *The Ore Minerals and Their Intergrowths.* Pergamon, New York.

Roedder, E. (1968). The noncolloidal origin of "colloform" textures in sphalerite ores. *Econ. Geol.* **63**, 451–471.

Stanton, R. L. (1972). *Ore Petrology.* McGraw-Hill, New York.

Taylor, L. A. (1969). The significance of twinning in Ag_2S. *Am. Mineral.* **54**, 961–963.

Vokes, F. M. (1969). A review of the metamorphism of sulphide deposits. *Earth. Sci. Rev.* **5**, 99–143.

Wiggins, L. B., and Craig, J. R. (1980). Reconnaissance of the Cu-Fe-Zn-S system: sphalerite phase relationships. *Econ. Geol.* **75**, 742–752.

Yund, R. A., and McCallister, R. H. (1970). Kinetics and mechanisms of exsolution. *Chem. Geol.*, 5–30.